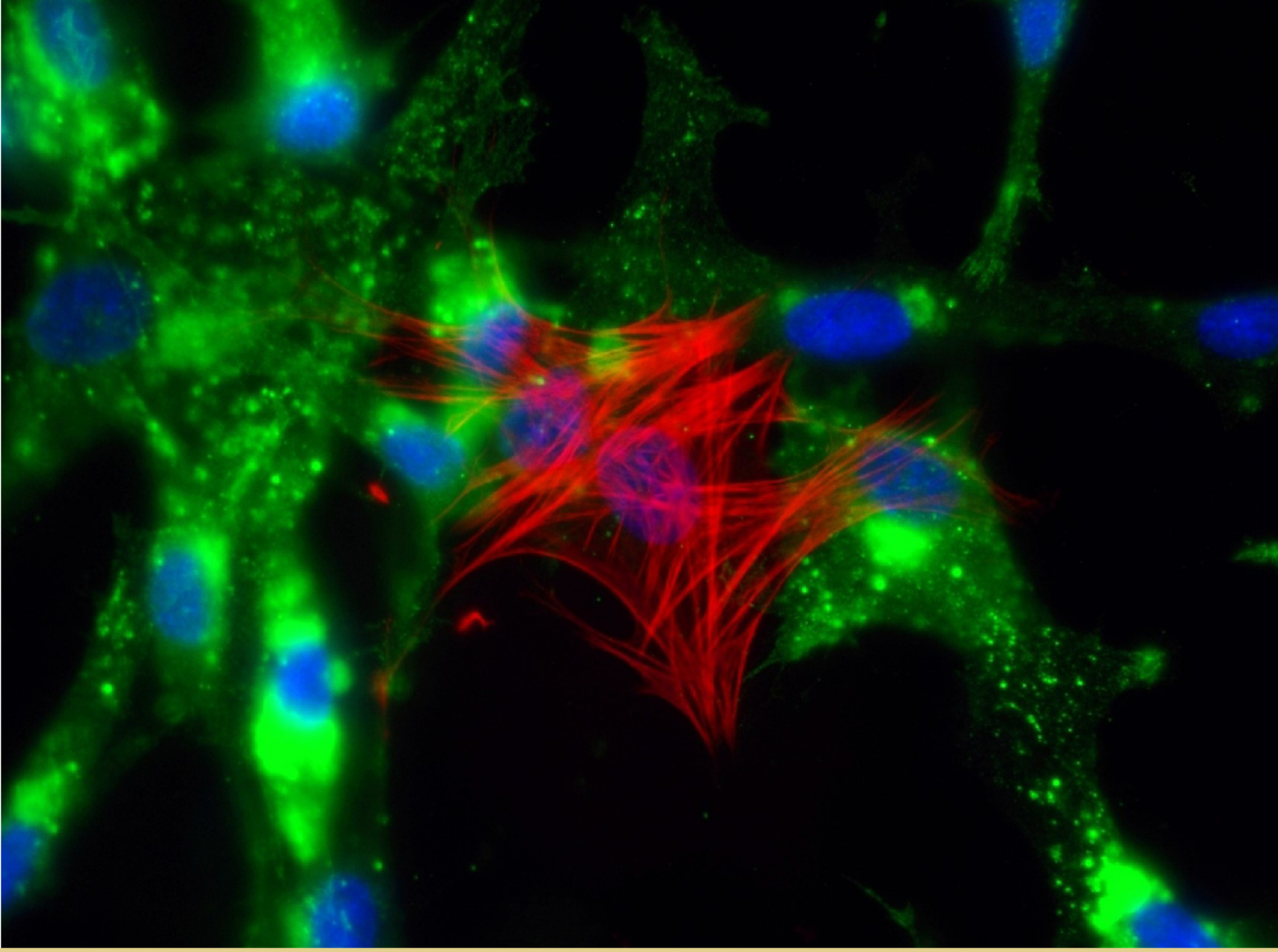

Salomé Isabel Marques Milagres

Two is better than one:
A combined therapy to prevent in-stent restenosis

Tese de Mestrado em Investigação Biomédica,
orientada pelo Doutor Henrique Girão e pela Doutora Elisabete Jorge
e apresentada à Faculdade de Medicina da Universidade de Coimbra

Julho 2018

· U C ·

Universidade de Coimbra

Two is better than one:

A combined therapy to prevent in-stent restenosis

Dissertação de Mestrado em Investigação Biomédica, na especialidade de Ciências da Visão apresentada à Faculdade de Medicina da Universidade de Coimbra para obtenção do grau de Mestre.

Orientadores: Doutor Henrique Girão e Doutora Elisabete Jorge

Coimbra, 2018

UNIVERSIDADE DE COIMBRA

O trabalho apresentado nesta dissertação foi realizado no Coimbra Institute for Clinical and Biomedical Research (iCBR) da Faculdade de Medicina da Universidade de Coimbra, sob a orientação do Doutor Henrique Manuel Paixão dos Santos Girão e co-orientação da Doutora Elisabete Sofia Azenha Balhau Jorge, no âmbito do Mestrado em Investigação Biomédica (MIB) da Faculdade de Medicina da Universidade de Coimbra.

Gostaria de dedicar esta tese aos meus pais, pelo apoio incondicional e pelas palavras certas no momento certo. Obrigada por me encorajarem a ser cada dia melhor. Se hoje sou quem sou, devo-o a vocês. Obrigada do fundo do coração.

Agradecimentos

Em primeiro lugar, ao Professor Henrique, meu orientador, por me ter recebido de braços abertos nos G(u)ic e pela confiança depositada em mim. Obrigada por ter sido sempre incansável comigo e por ter a porta do gabinete sempre aberta para as dúvidas (às vezes existenciais) da Poca. Agradeço-lhe também por todas as discussões científicas e por, no verdadeiro sentido da palavra, me ter orientado, diga-se, excecionalmente, durante esta fase da minha vida. Obrigada por todos os ensinamentos que me transmitiu. Cresci imenso consigo e tenho-o como exemplo de dedicação. Por último, mas não menos importante, obrigada pela boa disposição contagiante até porque "Sorri sempre…".

À Doutora Elisabete Jorge, minha co-orientadora, agradeço todo o apoio. Agradeço também por ser um modelo a seguir e o exemplo de que a investigação básica faz ainda mais sentido quando é aliada ao que se passa para lá da bancada do laboratório.

À Teresita, à minha Professora Teresa. A ti tenho-te a agradecer teres estado sempre ao meu lado desde o início e por todas as horas que despendeste comigo, muitas vezes, fora de horas. Obrigada por todos os ensinamentos e pela paciência mas também pelas confidências e desabafos. Foste sem dúvida um grande pilar durante este ano. Um grande obrigada.

À minha Dani. Obrigada pelas palavras de carinho, por toda a tua ajuda e pela tranquilidade que me transmitiste (tranqui!). Agradeço-te por te preocupares sempre comigo, pelas nossas conversas e pela amizade que fomos construindo. Muito obrigada por tudo Danizita.

Ao Steve. Agradeço-te imenso por tanto me teres ajudado ao longo deste ano e por seres sempre tão atencioso comigo. Ah, e espero que a sopa continue a constar no menu do almoço!

À Tânia, por toda a ajuda que me deste e pela tua honestidade. E claro, não é com qualquer pessoa que se partilha "Uma aventura no matadouro"!

À Mónica. A ti agradeço-te acima de tudo a tua amizade e os teus sábios conselhos. Foste um verdadeiro ombro amigo.

Às minhas companheiras de luta, à Jules e à Sofs. Obrigada por todas as piadas, gargalhadas, finos e alvarinhos. Obrigada pela companhia nas horas tardias e de (algum) desespero. Fico muito feliz pela amizade "incriveu" que nos uniu.

Ao Jorgito, pelo carinho, preocupação e pelas palavras certas no momento certo. E claro, obrigada por me avisares sempre quando estou fora da graça de Deus.

À Carla e à Elisa, por toda a paciência comigo e por todos os ensinamentos.

À Raquel e à Patrícia, pelos cafés infindáveis e pelos desabafos nos momentos mais difíceis. De facto, o MIB junta pessoas incríveis e eu só tenho a agradecer por vos ter encontrado.

Aos de sempre, aos amigos de Cantanhede. Obrigada por todo o incentivo e desculpem a ausência. À Batiz e à Melo, por tão longe, estarem sempre tão perto. À Marisa, pelas cafezadas e gargalhadas noite fora.

Aos que não são de sempre mas vão ficar para sempre. À Costinha, obrigada pela paciência e por todos os "vamos aos finos por favor". À Bibi, pela tua presença e por todos os "vamos lá abaixo por favor". E ao Cardoso, por todas as gargalhadas serem sempre tão fáceis contigo. Pode ser o maior dos clichés, mas levo-vos comigo para a vida.

À Xandra, por todo o carinho e paciência comigo. Nunca to disse, mas és como uma irmã para mim. Ao Joãozito. Quando cresceres conto-te a força que deste à Mimi. Ao Gustavo. Quando cresceres, também te conto como o teu sorriso me recarregava as baterias. À Titi, por acreditares sempre em mim e por acenderes aquela velinha nos momentos de aflição. Mas no final de contas, "força aí galera"! À Vovó. Espero que estejas orgulhosa de mim. Talvez um dia venha mesmo a ser uma grande doutora.

Ao David, por teres estado sempre ao meu lado e também nesta fase da minha vida. Obrigada pelo carinho, pela preocupação e por toda a força. Por simplesmente ouvires a Mecas quando assim tinha de ser e por compreenderes as horas infindáveis passadas no laboratório. O resto, tu sabes.

Ao meu irmão. Obrigada por tudo Nikinhas! Obrigada por me ensinares tanto e por seres um pilar tão grande na minha vida e desculpa o mau feitio às vezes. Obrigada por seres um companheiro, um amigo. Devo-te tanto…

Por fim, dirijo um agradecimento especial aos meus pais, por serem para mim o exemplo de valores, coragem, perseverança e de que, quando se quer, tudo se consegue, basta acreditar em nós próprios. Afinal de contas, a sorte dá mesmo muito trabalho. Obrigada pelo apoio incansável, pelas palavras de força e, acima de tudo, por serem o meu suporte. Agradeço-vos tudo o que fizeram por mim e claro que nada disto seria possível sem vocês. Um grande obrigada do fundo do coração.

Table of contents

Index of Figures

Abreviations

AMPK	AMP-activated protein kinase
ATGs	Autophagy related genes
Baf A	Bafilomycin A1
BMS	Bare-metal stent
BSA	Bovine serum albumin
CABG	Coronary artery bypass grafting
CAD	Coronary artery disease
CVD	Cardiovascular diseases
Cx	Connexin
Cx43	Connexin43
DES	Drug-eluting stent
DMEM	Dulbecco's Modified Eagle Medium
EC	Endothelial cells
ECGF	Endothelial cell growth factor
ECM	Extracellular Matrix
EPC	Endothelial progenitor cells
FBS	Fetal bovine serum
FKBP12	FK506-binding protein 12
GJ	Gap junctions
HBSS	Hank's Balanced Salt Solution
HMG-CoA	3-hydroxy-3-methylglutaryl-CoA
HRP	Horseradish peroxidase
PAEC	Human pulmonary arterial endothelial cells
p-mTOR	Phospho-mTOR
ISR	In-stent restenosis
LC3	Microtubule-associated protein 1 light chain 3
LDL	Low-density lipoprotein
Leup	Leupeptin
LSGS	Low Serum Growth Supplement

MCEC-1	Mouse cardiac endothelial cell line
mTOR	Mammalian target of rapamycin
MTT	[3-(4,5-dimethylthiazol-2-yl)-2,5-diphenyl-2H-tetrazolium bromide]
PBS	Phosphate-buffered saline
PCI	Percutaneous coronary intervention
PE	Phosphatidylethanolamine
PFA	Paraformaldehyde
PI3K	Phosphoinositide-3-kinase
SDS-PAGE	Sodium dodecyl sulfate polyacrylamide gel electrophoresis
SES	Sirolimus-eluting stent
Simv	Simvastatin
SMC	Smooth muscle cells
TBS-T	Tris-buffered saline-Tween 20
ULK1	Unc-51-like kinase 1
UPS	Ubiquitin-proteasome system
WB	Western blot

Resumo

As doenças cardiovasculares são a principal causa de morte, em todo o mundo, sendo a doença arterial coronária a mais comum, causada pela diminuição do fluxo sanguíneo na sequência de uma oclusão, total ou parcial, das artérias coronárias. O tratamento da doença arterial coronária é geralmente realizado por meio de uma intervenção coronária percutânea, na qual, através de uma angioplastia de balão, um stent é implantado dentro da artéria coronária para evitar a sua estenose. No entanto, a insuflação do balão exerce elevadas pressões contra a parede, resultando na desnudação do endotélio e na hiperplasia da neoíntima, caracterizada pela proliferação de células do músculo liso na túnica intima. Os stents eluídos com sirolimus, um análogo da rapamicina e um potente agente citostático, provaram ser eficazes a prevenir a migração e proliferação de células do músculo liso. No entanto, o sirolimus leva à disfunção endotelial e suprime a capacidade de reendotelização da coronária, o que pode causar a reestenose em stent. A sinvastatina é uma estatina rotineiramente utilizada na prática clínica devido às suas propriedades em inibir a 3-hidroxi-3-metilglutaril-CoA redutase, bloqueando assim a síntese do colesterol. Uma vez que a sinvastatina demonstrou ser capaz a inibir a proliferação de células do músculo liso e tem sido descrita possuir efeitos protetores na migração e proliferação de células endoteliais, neste estudo propomos que o efeito deletério do sirolimus no contexto da reestenose em stent pode ser revertido pela terapia combinada da rapamicina e sinvastatina.

Neste trabalho, avaliou-se o efeito da rapamicina e/ ou sinvastatina na migração, proliferação, potencial angiogénico e atividade autofágica de dois tipos de células endoteliais, nomeadamente, MCEC-1, uma linha celular de células endoteliais cardíacas de murino e PAEC, células endoteliais primárias de artérias pulmonares de humano.

Os resultados obtidos neste estudo demonstraram que a inibição da migração em MCEC-1 induzida pela sinvastatina pode ser parcialmente revertida pela rapamicina, enquanto que em PAEC, a rapamicina não demonstrou melhorar o efeito inibitório da sinvastatina na migração. No entanto, observámos uma tendência para doses mais altas de sinvastatina aumentar a migração.

Em relação à proliferação, as taxas de proliferação de MCEC-1 não foram alteradas nem pela rapamicina nem pela sinvastatina ao passo que, em PAEC, a incubação com sinvastatina, na presença ou ausência de rapamicina, reduziu a capacidade de proliferação

destas células. Uma vez mais, PAEC demonstraram uma propensão para responderem melhor sob doses mais elevadas de sinvastatina.

Através de ensaios de tubulação *in vitro*, o nosso estudo mostrou que o tratamento de MCEC-1 com rapamicina induz uma redução na capacidade angiogénica destas células, que podia ser revertida pela sinvastatina. Por outro lado, em PAEC, nem a sinvastatina nem a rapamicina afectaram a formação de estruturas capilares semelhantes a novos vasos, sugerindo que estes compostos não interferem com a capacidade angiogénica destas células. No entanto, uma dose maior de sinvastatina não foi testada.

Além disto, também avaliámos o efeito destes compostos na modulação da resposta autofágica das células endoteliais e do músculo liso. Com base nos resultados que mostram a acumulação de p62 e LC3-II na presença de um inibidor do lisossoma, demonstramos que tanto as células endoteliais como as do músculo liso apresentam uma elevada atividade autofágica basal. Além disso, a Conexina 43, um substrato de autofagia, também é acumulada.

Este estudo permitiu ainda demonstrar que abordagens "clássicas" para modular a autofagia, como é o caso da privação de soro ou de aminoácidos, ou o tratamento com rapamicina, levam também a uma ativação da autofagia nas MCEC-1.

No que diz respeito ao efeito da sinvastatina na modulação da autofagia nas células endoteliais estudadas, demonstramos que este efeito é diferente em MCEC-1 e PAEC. De facto, os nossos resultados sugerem que a maquinaria de autofagia envolvida varia de acordo com o tempo de indução de autofagia, sendo numa primeira fase dependente de AMPK, enquanto que para períodos mais longos a Beclina-1 parece ter um papel preponderante. Com base nos resultados a mostrar que o efeito, em termos de níveis de LC3-II, da sinvastatina na presença de bafilomicina é semelhante ao efeito da bafilomicina isolada, sugerimos que a sinvastatina inibe a fusão do autofagossoma com o lisossoma.

Em células do músculo liso, a sinvastatina não induziu um efeito na atividade autofágica nas primeiras 24 horas, enquanto que para incubações de 48 horas se verificou uma diminuição dos níveis de LC3-II, sugerindo que uma estimulação da autofagia.

Este estudo demonstra que o efeito da rapamicina e da sinvastatina na migração, proliferação e capacidade angiogénica varia consoante o tipo de célula endotelial e que estes compostos exercem impactos diferentes na autofagia das células estudadas.

Abstract

Cardiovascular diseases (CVD) are the leading cause of death worldwide, being coronary artery disease (CAD) the most common one, caused by a shortage of blood supply to the heart due to partial or total occlusion of coronary arteries. The treatment of CAD usually involves percutaneous coronary intervention (PCI), in which, through a balloon angioplasty, a stent is implanted within the coronary artery to prevent its stenosis. The balloon insufflation, however, exerts high pressures against the wall resulting in endothelial denudation and consequent neointima hyperplasia, characterised by the proliferation of smooth muscle cells (SMC) within tunica intima. Stents eluted with sirolimus (SES), an analogue of rapamycin and a potent cytostatic agent, have proven efficient arresting SMC migration and proliferation. Nevertheless, sirolimus leads to endothelial dysfunction and supresses re-endotheliazation capacity of the coronary, which may cause in-stent restenosis (ISR). Simvastatin is a statin routinely used in clinical practice due to its properties to inhibit 3-hydroxy-3-methylglutaryl-CoA (HMG-CoA) reductase, thus blocking cholesterol synthesis. Since simvastatin has proven able to inhibit SMC proliferation and has been described to hold protective effects in migration and proliferation of endothelial cells (EC), in this study we propose that the deleterious effect of sirolimus in the context of ISR may be reverted by the combined therapy of rapamycin and simvastatin.

In this work, we assessed the effect of rapamycin and/ or simvastatin in migration, proliferation, angiogenic potential and autophagy activity of two types of EC, namely, MCEC-1, a mouse cardiac endothelial cell line, and PAEC, human pulmonary arterial endothelial cells.

The results obtained demonstrated that MCEC-1 cell migration inhibition caused by simvastatin can be partially reverted by rapamycin, whereas in PAEC, the incubation with rapamycin did not ameliorate the inhibitory effect of simvastatin in migration. However, we observed a tendency for higher doses of simvastatin to increase migration.

Regarding proliferation, MCEC-1 proliferation rates were not altered neither by rapamycin or simvastatin, whereas in PAEC, the incubation with simvastatin, in the presence or absence of rapamycin, impaired proliferation capacity of these cells. Once more, PAEC demonstrated a propensity to response better under higher doses of simvastatin.

Using tube formation in vitro assays, our work showed that MCEC-1 treatment with rapamycin induced a decrease in the angiogenic capacity of these cells, which could be reverted by simvastatin. On the other hand, in PAEC, neither simvastatin nor rapamycin affected the formation of capillary-like structures, suggesting that the angiogenic properties of these cells are not being affected by these compounds. However, a higher dose of simvastatin was not tested.

Furthermore, we evaluated the effect of these compounds in autophagic response of EC and SMC. Based on the results showing the accumulation of p62 and LC3-II in the presence of a lysosome inhibitor, we demonstrated that both EC and SMC present a high basal autophagic activity. In accordance, Connexin 43 (Cx43), an autophagy substrate, also accumulated. This study also established that approaches already known to be autophagy modulators, such as serum or amino acid deprivation, or treatment with rapamycin, also lead to an autophagy activation in MCEC-1.

Moreover, our study showed that the effect of simvastatin in autophagy is different in MCEC-1 and PAEC, suggesting this is a cell-specific response. Additionally, we demonstrated that the autophagy machinery involved varies according to the duration of autophagy induction, in a first stage being AMPK-dependent, while in longer periods Beclin-1 seems to have a preponderant role. Based in the results demonstrating that the effect, regarding LC3-II levels, of simvastatin in the presence of bafilomycin is similar to the effect of bafilomycin alone, we suggest that simvastatin inhibits the fusion of the autophagosome with the lysosome.

Regarding SMC, simvastatin did not affect autophagy activity in the first 24 hours of incubation, whereas in 48 hours of incubation it was observed a decrease of LC3-II levels, suggesting an autophagy stimulation.

This study demonstrates that the effect of rapamycin and simvastatin in cell proliferation, migration and angiogenesis capacity, is endothelial cell-type specific and that these compounds exert different impacts in the studied cell.

1. Introduction

1.1 The heart

Life, from the beginning, depends on the uninterrupted function of the heart. The main function of this muscular organ is to pump blood through the circulatory system, delivering nutrients and oxygen to all tissues and organs of the body. Within the four chambers of the heart, exist a variety of cell types and each one is essential to the maintain structural, biochemical, mechanical and electrical properties of the heart[1].

Unlike certain fish and amphibians that maintain a robust cardiac regeneration capacity throughout life, mammalian adult hearts do not possess the same levels of regeneration after an insult[1], developing instead a reparative response.

The heart can repeatedly and rhythmically contract and relax and this contractile capacity relies on the myocardium, the cardiac muscle. The presence of specialized cardiomyocytes called Pacemaker cells that hold intrinsic depolarization properties is what mainly dictates the rhythm of the heartbeat. For the heart to contract as a syncytium, the electrical impulses generated at the Pacemaker cells must be rapidly and efficiently propagated to the rest of myocardium. Indeed, in order for the heart work in a synchronized and coordinated manner, it depends on the existence of intercellular low resistance channels called gap junctions (GJ).

1.1.1 Connexin 43

These specialized cell-to-cell junctions are formed by six subunits of a protein called connexin (Cx) responsible for ensuring the rapid and efficient anisotropic electrical signal propagation. The Cx family encloses 21 described members and several of them are expressed in the heart[2], of these, connexin 43 (Cx43) is the most expressed[3]. Therefore, Cx43 expression levels give important information to understand how cell-cell communication is occurring.

1.1.2 Coronary artery wall histology

The purpose of coronary arteries and their derived branches is to supply the heart with blood, thus being responsible for all the coronary circulation.

Coronary artery wall organization is very well established as a three-layer structure: an external layer, the adventitia layer or tunica adventitia; a middle layer, the medial layer or tunica media and an inner luminal layer, the intima layer or tunica intima. Briefly, the tunica adventitia is constituted by fibrous tissue namely elastic fibers and collagen and is surrounded by lymphatic vessels, nerves and vasa vasorum, a network of small blood vessels that provide blood and nourishment supply to larger blood vessels[4].

The tunica media comprises up to 40 layers of smooth muscle cells (SMC) and connective tissue constituted by collagen and proteoglycans[4]. Unmyelinated nerve axons from the external layer stimulate SMC present in the media, and the subsequent depolarization of these SMC is propagated through low resistance GJ[5]. The thickness values of a normal tunica media ranges from 125 to 350 µm but when the intima layer is compromised, for instance due to the presence of an atherosclerotic plaque, the tunica media can become thinner ranging from 16 to 190 µm[6].

Closer to the lumen, the intima possesses a lining layer of endothelial cells (EC) and a subendothelial layer mainly constituted by connective tissue. Arteries and more particularly the EC are uninterruptedly exposed to the passage of blood and, consequently subjected to hemodynamic forces and shear stress, frictional tangential forces that act on the endothelial surface[7]. To cope with these continuous tensions, the EC are longitudinally oriented to the artery and strongly attached to each other through GJ. Overall, the endothelium provides an important selective diffusion barrier between the blood and the adjacent layers and the resident EC display important functions, namely the production of inflammatory mediators such as interleukin-1, growth factors (platelet-derived growth factor), antithrombotic agents but also prothrombotic agents like the von Willebrand's factor, and contain receptors for low

density lipoprotein (LDL)[8]. Taking this into account, the endothelium can be accepted as the gatekeeper of artery health[7].

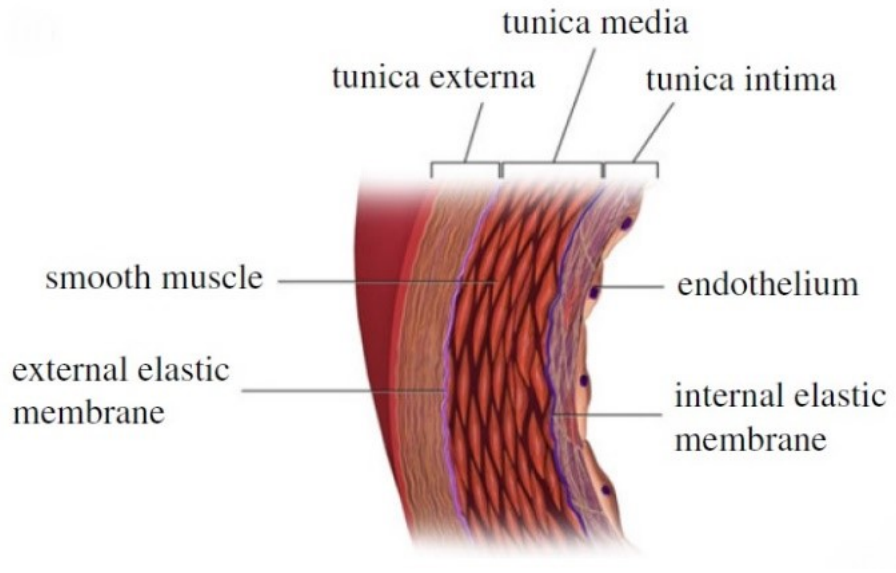

Figure 1. Schematic representation of the coronary artery wall.
The artery wall is composed by three layers: tunica externa, tunica media and tunica intima and elastic membranes separating them. Adapted from: Melnikova, N. B., et al. (2017).

1.2 Cardiovascular disease

Since the heart has to beat non-stop, it is easily understandable that an insult can have catastrophic consequences. Despite all the advances in the field, cardiovascular disease (CVD) still represents a massive economic burden and remains the major cause of mortality and morbidity worldwide, accounting for one third of CVD related deaths occurring before 75 years of age, less than the average life expectancy. In the last years, the world has witnessed an increase in population ageing speed and, consequently, a growing life expectancy. However, this higher longevity is not a causal relationship to good quality of life. For instance, CVD represents a huge increase in lifetime risk, above 60%, and a significant decrease in patient quality of life[9].

1.2.1 Cardiovascular disease: an ageing disease

CVD is truly a disease of ageing. The progressive decline of microvascular homeostasis and impairment of angiogenic processes are closely associated with advanced ageing[10]. This diminished capacity of EC to form new vascular structures is triggered by changes in core signalling pathways, thus affecting processes like adhesion, migration, extracellular matrix (ECM) turnover, release of growth factors and cytokines SMC recruitment and vessel stabilization[11]. Moreover, circulating endothelial progenitor cells (EPC) which are responsible for generating new EC, have been reported to play important roles in angiogenesis stimulated by coronary artery disease (CAD) and to be less functional in old age[12,13]. In elderly people, endothelial dysfunction plays a critical role since senescent endothelial cells do not proliferate, and their angiogenic capacity is compromised[14].

Although the heart is a remarkably resilient organ, endothelial dysfunction and deficient angiogenesis compromises the recovery after tissue damage. Therefore, strategies that can, even partially, restore vascular flow after artery blockage are vital to preserve blood supply. This plays a crucial role in percutaneous coronary intervention (PCI) with balloon angioplasty which is the standard procedure to treat CAD, one of the most common forms of CVD.

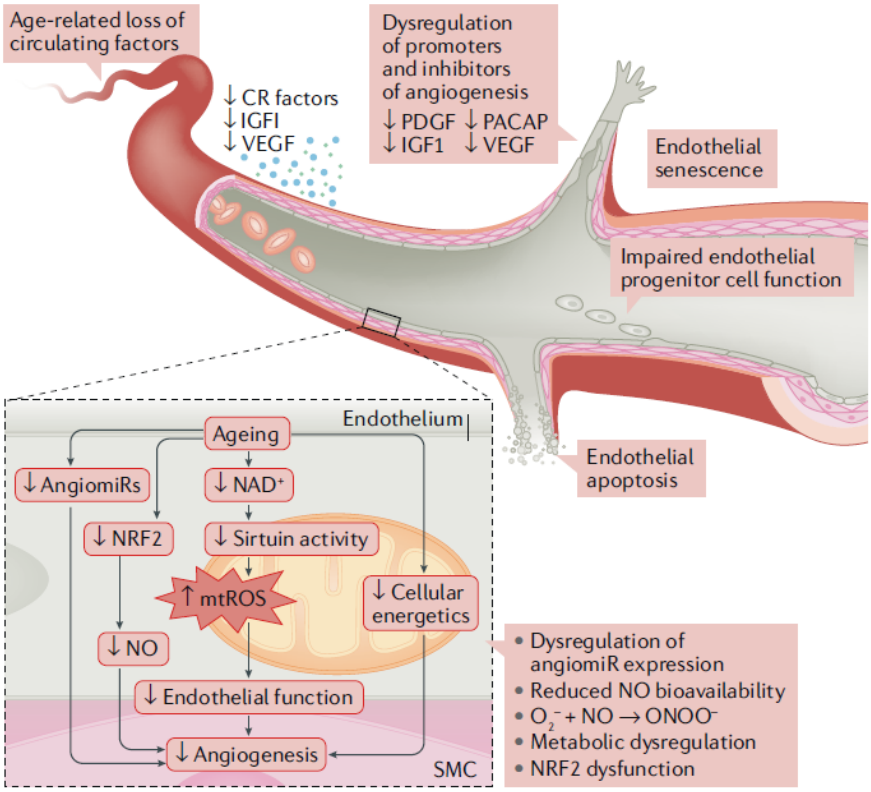

Figure 2. Impaired endothelial function in ageing.
Advanced ageing progressively deteriorates microvascular homeostasis and impairs endothelial cell intrinsic functions. The underlying mechanisms are endothelial senescence and dysfunction, impaired angiogenic potential and endothelial progenitor cell function and increased endothelial apoptosis. From: Ungvari, Z. et al. (2018).

1.3 Coronary artery disease

Among all CVDs, CAD is the one claiming more deaths. Being the most common form of CVD, CAD is responsible for one in every seven deaths worldwide[15]. From a clinical point of view, the extent and severity of coronary artery stenosis has been correlated with long-term mortality[16].

1.3.1 Atherosclerosis

Atherosclerosis is a chronic inflammatory disease and is the main pathologic condition underlying CAD. This pathology is characterized by the localized accumulation of cholesterol, macrophages and SMC inside the arteries over many decades and as a result the artery intimal area thickens, eventually restricting blood flow, a process called

stenosis. Atherosclerotic plaques are typically found in arterial branch points and other regions of altered hemodynamic due to disturbed laminar blood flow patterns in these regions[17,18].

The complex etiology of atherosclerosis begins with perturbations in the endothelium which, through the slow accumulation of lipoproteins within the subendothelial space, ultimately results in severe changes in the protective role of the endothelial lining[7]. Under pathological conditions, the endothelium becomes inflamed and leaky[19] which allows monocyte infiltration and its differentiation into macrophages, and not only decreases EC capacity to regenerate[20] but also enhances their apoptosis. Since the endothelium becomes compromised, LDL particles are now able to cross the endothelial monolayer. Once there, those LDL particles are oxidized and become foam cells[21] and that is just the trigger SMC needed to migrate in direction to the intima, where they proliferate and deposit ECM like collagen and elastin[7]. This phenomenon occurs through matrix remodelling and calcification[22]. These escalated events culminate with an atherosclerotic plaque enriched in inflammatory cells which will contribute to the endothelial proinflammatory phenotype and to further structural instability of the plaque[23].

In fact, the endothelial monolayer can be accepted as the first line of defense against atherosclerosis, but once it becomes compromised and dysfunctional atherosclerosis will persevere[7].

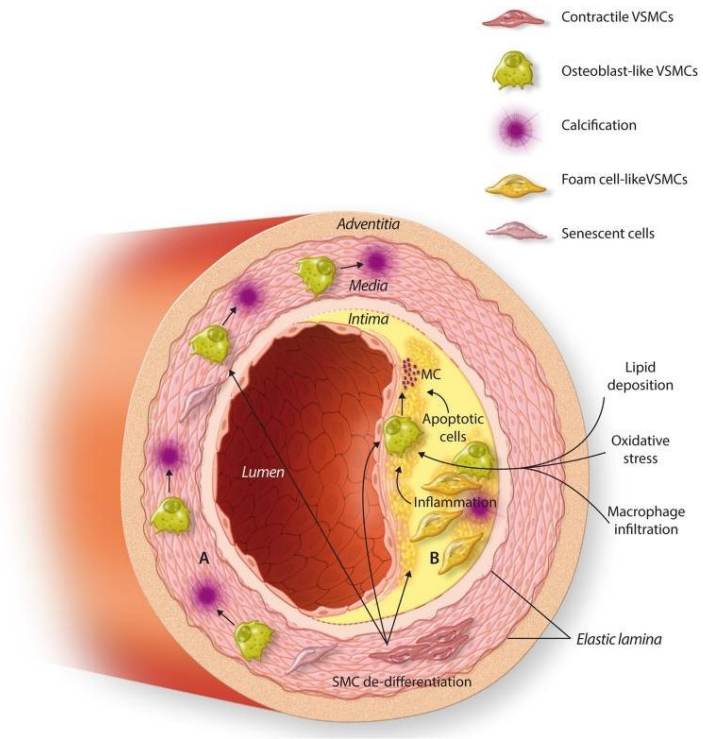

Figure 3. Formation of an atherosclerotic plaque.
(A) Within the tunica media, SMC triggered by osteogenic stimuli differentiate into osteoblast-like cells. Subsequently calcification of the medial layer blood vessels leads to artery wall stiffening. (B) Atherosclerosis is characterized by lipid deposition between media and intima layers, allowing macrophage infiltration and SMC differentiation into foam cells. Inflammation, apoptosis, and oxidative stress occurs and SMC acquire an osteoblast-like cells phenotype. Calcification occurs within the intima wall, which weakens the artery and increases plaque instability and consequent risk of plaque rupture. From: L. Durham, A.L. et al. (2018).

1.4 Coronary artery disease treatment

For many years, the standard treatment for CAD was coronary artery bypass grafting (CABG), in which a healthy vessel from another part of the body is grafted into the narrowed artery, bypassing the blocked region and creating a new route to supply that area. Because CABG is an invasive surgery with slow recovery and serious associated morbidity, percutaneous coronary intervention (PCI) presented an alternative to provide relief to patients subjected to CABG[15].

1.4.1 Balloon angioplasty

Balloon angioplasty is delivered through a medical procedure called PCI usually via the common femoral artery[24]. In this technique, a catheter attached to a deflated balloon conducted by a guide-wire is directed to the stenotic area where the balloon is inflated. The expansion compresses the atherosclerotic plaque, increases the arterial lumen

calibre[24] and restores adequate blood flow. To ensure the balloon opens to the appropriate size, it must be insufflated with 6 to 20 atmospheres which corresponds to 75 up to 500 times the normal blood pressure.

In the last decades, approaches regarding PCI with balloon angioplasty evolved a lot with the development of improved techniques and materials but more importantly with the introduction of bare-metal stents (BMS) in 1986 and drug-eluting stents (DES) in 1999[25]. Nowadays, PCI in the form of balloon angioplasty with stent delivery is the most common procedure to treat CAD patients[26].

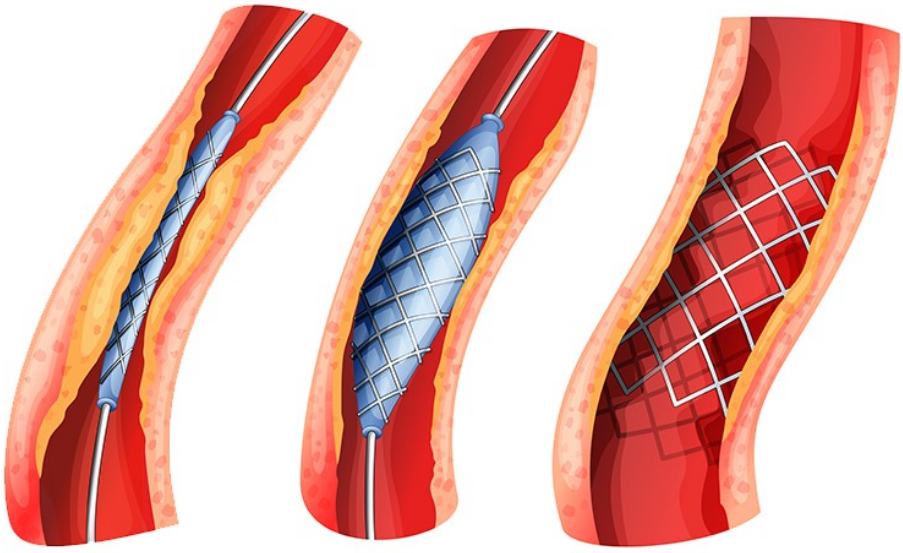

Figure 4. Balloon angioplasty followed by stent implantation.
In order to treat atherosclerosis, a stent collapsed around the balloon at the tip of the catheter can be guided to the blocked artery. At the narrowed area, the balloon is inflated destroying the accumulated atherosclerotic plaque and the stent is expanded, further supporting the walls of the artery to help prevent restenosis. Accessed 27 June 2018, adapted from <https://www.medtechintelligence.com/feature_article/how-to-ce-mark-a-medical-device-that-incorporates-a-drug/>.

1.4.2 In-stent restenosis

A stent is a tube-shaped device composed by metal meshes used in interventional cardiology to open an occluded artery and that stays juxtaposed to the arterial wall. BMS, composed by metal only, were the first devices introduced in coronary stenting[27]. Despite BMS reducing the rates of restenosis compared with balloon angioplasty, in-stent restenosis (ISR), the narrowing within the stented section, still developed in 20 to 30% of the cases[27].

ISR is the natural healing response of the arterial wall to the mechanical injury[28] inflicted by the BMS. This phenomenon relies on the high pressures exerted against the artery wall when the stent is expanded, resulting in scar formation.

Insufflate the stent immediately starts a cascade of events, namely stretch of the entire artery, rupture of the plaque often followed by dissection into the media and sometimes adventitia[29] and the denudation of the endothelium. Resident macrophages stimulate leukocytes migration and growth factors release from SMC, triggering these cells to migrate from the media to the intima. Although under normal conditions SMC are quiescent and possess diminished proliferative levels, mechanical injury and growth factors trigger them to enter in the cell cycle[30]. This is partially due to the absence of EC, removed by balloon inflation, since one of the main biological functions of EC is to repress SMC proliferation. As a result, a new postinjury layer inside the lumen starts to develop, the neointima[31], enriched with SMC, macrophages and ECM. Moreover, further cellular division starts to take place within the neointima and through long periods of time SMC proliferate, culminating in neointimal hyperplasia[28]. Along with this increase in neointimal thickness, the artery also undergoes a remodelling phase characterized by ECM reorganization, thus degrading cellular components and replacing it with collagen. An increased deposition of ECM and the hyperplasia of the neointima can ultimately lead to the shrinkage of the entire artery[29].

As a conclusion, endothelium denudation is the driving force towards neointimal hyperplasia. Indeed, tunica intima integrity is vital to maintain vascular homeostasis, and because EC population is largely decreased after stent inflation, the injured endothelium is not able to inhibit SMC growth[32].

1.4.3 Drug-eluting stents

The development of stents eluted which slowly release antiproliferative and anti-inflammatory drugs, DES, was a major breakthrough in ISR treatment[33]. Because DES mainly target SMC proliferation and consequently neointima hyperplasia, ISR incidence dropped drastically compared to BMS. However, this approach also presents some drawbacks. In fact, several reports of late stent thrombosis started to be described[34], emerging as a serious complication that often leads to myocardial infarction and death[35].

Late stent thrombosis relies on the two-faced properties of DES. The antiproliferative compounds not only inhibit SMC proliferation but also inhibit proper re-endotheliazation, that contributes to delayed arterial healing[36]. ISR still develop in 8-20% of patients[37] and from a clinical point of view it constitutes the main limitation to stent implantation[36].

1.4.4 Sirolimus-eluting stents

Regarding drug pharmacokinetics, the ideal compound should on one hand ensure the delivery of high local concentrations, but on the other hand also ensure a homogeneous diffusion[38]. Among the several drugs used in DES, sirolimus, an analogue of rapamycin, is one of the most popular ones. Sirolimus-eluting stents (SES) demonstrated to have an even distribution of sirolimus through the artery, compared with other drugs[38].

However, a proper re-endotheliazation within the stented area is crucial to the short and long-term success of stent implantation[39]. And this is precisely where sirolimus stumbles. Although this drug decreases neointimal thickening by inhibiting SMC migration and proliferation[40], it also impairs the healing process of the denudated artery[41], the primary reason for DES thrombosis[42].

1.5 Rapamycin

Also known as sirolimus, rapamycin is a natural drug isolated from *Streptomyces hygroscopicus* and was discovered in the 1970s. Rapamycin possesses strong cytostatic effects because it selectively induces cell cycle arrest in the late G1 phase[43], blocking cytokinesis progression. Due to its potent immunosuppressive and cytostatic properties, rapamycin is the most common drug applied to induce autophagy.

Although it drew the immediate attention of clinicians and scientists[44], the poor solubility of rapamycin restrained its use[45]. Therefore, analogues started to be developed and tested as antirestenotic agents, like Everolimus and Zotarolimus[28].

But rapamycin is not like all the other drugs. Contrary to other immunosuppressors that only inhibit DNA synthesis, rapamycin has the capacity to bind to the FK506-binding protein 12 (FKBP12), a protein that is found upregulated in SMC

from the neointima[43]. This FKBP12/Rapamycin complex binds to the mammalian target of rapamycin (mTOR), a crucial protein in cell cycle regulation, and inhibits it[28].

1.5.1 My name is TOR, mTOR

TOR is a member of the phosphoinositide-3-kinase (PI3K)-related protein kinase family which is known to be heavily involved in the cell cycle[46]. mTOR is the mammalian form and is a serine/threonine-protein kinase responsible for sensing cellular nutrient status, thus working as a master regulator of cell metabolism[47] and autophagy. More particularly, mTOR regulates the transition between the G1 and S phase[28], therefore playing a crucial role in cellular division and cell cycle progression.

mTOR truly works as a master regulator of cell growth, proliferation and migration. It comprises two complexes, the mTORC1 and the mTORC2. The last one is relatively unresponsive to rapamycin while mTORC1 is highly sensitive and directly regulates autophagy[48]. Complex mTORC1 is responsible for the maintenance of autophagy basal levels since it phosphorylates the autophagy kinase complex ULK1/2, leading to phagophore formation. However, if mTORC1 is inactivated by rapamycin for example, the mTORC1:ULK1/2 complex dissociates and autophagy is activated[49].

1.6 Autophagy

A healthy proteome relies on multiple regulatory mechanisms, but generally balanced proteostasis ensures an efficient protein quality control that is crucial for cellular homeostasis. Chaperones and the ubiquitin-proteasome system are the first line of defence but if things go wrong and this protein quality control fails, macroautophagy jumps on to the stage[50].

Macroautophagy, commonly referred to as autophagy, is a highly conserved catabolic process that takes advantage of very specialized machinery to engulf cargo for lysosomal degradation. Autophagy substrates comprises proteins, lipids, nucleic acids, pathogens and damaged organelles[51], providing materials for ATP production, protein synthesis and gluconeogenesis, allowing cell survival. On the other hand, excessive or dysfunctional autophagy may lead to cell death[52].

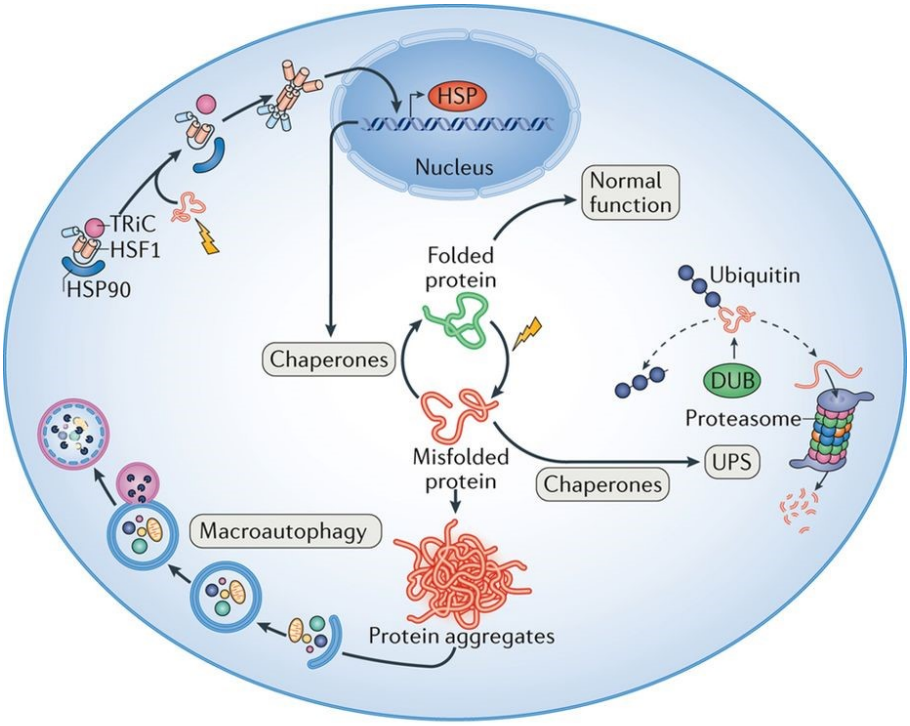

Figure 5. Overview of the protein quality control system.
Stress causes protein misfolding or damage in functional proteins, often resulting in exposure of hydrophobic surfaces. Chaperones binds and refold these damaged proteins. However, when refolding is not an option, chaperones keep the misfolded protein in a soluble state available to protein-degradation systems. The ubiquitin–proteasome system (UPS) is the first system responsible for degradation soluble misfolded, oxidized or otherwise-damaged proteins. If proteins cannot be maintained in a soluble state, autophagy is an alternative pathway to clear protein aggregates. From: Henning, R. H., et al. (2017).

1.6.1 Mechanisms of autophagy

1.6.1.1 Help, I am stressed out!

Cellular stress, like growth factor depletion, infection, hypoxia or starvation[44], quickly triggers an adaptive response in the cell in the form of autophagy and more particularly, during periods of starvation autophagy recycles damaged cellular components to provide the cell with nutrients that ensure its vital processes[44]. Indeed, deprivation of amino acids is the most common way to induce autophagy since it inhibits mTOR activity[53].

Another way to induce autophagy is through AMP-activated protein kinase (AMPK) activation. AMPK is a master regulator of cellular metabolism[54] and is recruited under stress conditions. In response to mitochondrial damage and low ATP levels, AMPK is activated[51] and directly phosphorylates mTOR upstream regulators[55], whose phosphorylation then reduces mTOR activity. Since mTOR activity is now reduced, the

inhibitory phosphorylation on Unc-51-like kinase 1 (ULK1) is relieved and autophagy is activated.[51] Interestingly, some evidences suggest that AMPK pharmacological activation produces protective effects in EC[56].

1.6.1.2 A cascade of events

Since we are talking about a tightly controlled process, the machinery necessary involves the recruitment of several multi-protein complexes[44].

Induction of autophagy starts with a stress signal and the recruitment of more than 30 autophagy related genes (ATGs) that will control the entire process. The first steps of autophagy are initiation followed by nucleation. Autophagy initiation can be triggered by different signalling pathways like hypoxia or starvation, and it starts when ULK1 complex phosphorylates members from the autophagy machinery, like Beclin 1. During nucleation, a cup-shaped membrane called phagophore is formed. In the elongation and closure step, the phagophore gradually elongates and eventually closes, forming a double-membrane vesicle called autophagosome that engulfs cytosolic components to be degraded. In this step, microtubule-associated protein light chain 3 (LC3) is conjugated to membrane-resident phosphatidylethanolamine (PE), resulting in the conversion of the cytosolic free form (LC3-I) into a lipidated form (LC3-II), a characteristic signature of autophagic membranes. Among other autophagy cargo receptors, LC3 and SQSTM1, also known as p62, are deeply involved in cargo sequestration. p62 is an autophagy receptor, binding to autophagy substrates and directing them to LC3-II in the nascent phagophore, mediating their autophagic sequestration and cargo degradation[57]. The autophagosome that now contains autophagic cargo goes through a maturation phase and ends up fusing with the lysosome and forming a new structure, the autophagolysosome. PE-conjugated LC3 also intervenes in autophagosome maturation and mediates autophagosome-lysosome fusion upon phosphorylation. This autophagolysosome together with the cargo trapped inside, are finally degraded by lysosomal enzymes and metabolic products are released to the cytoplasm to be recycled[44].

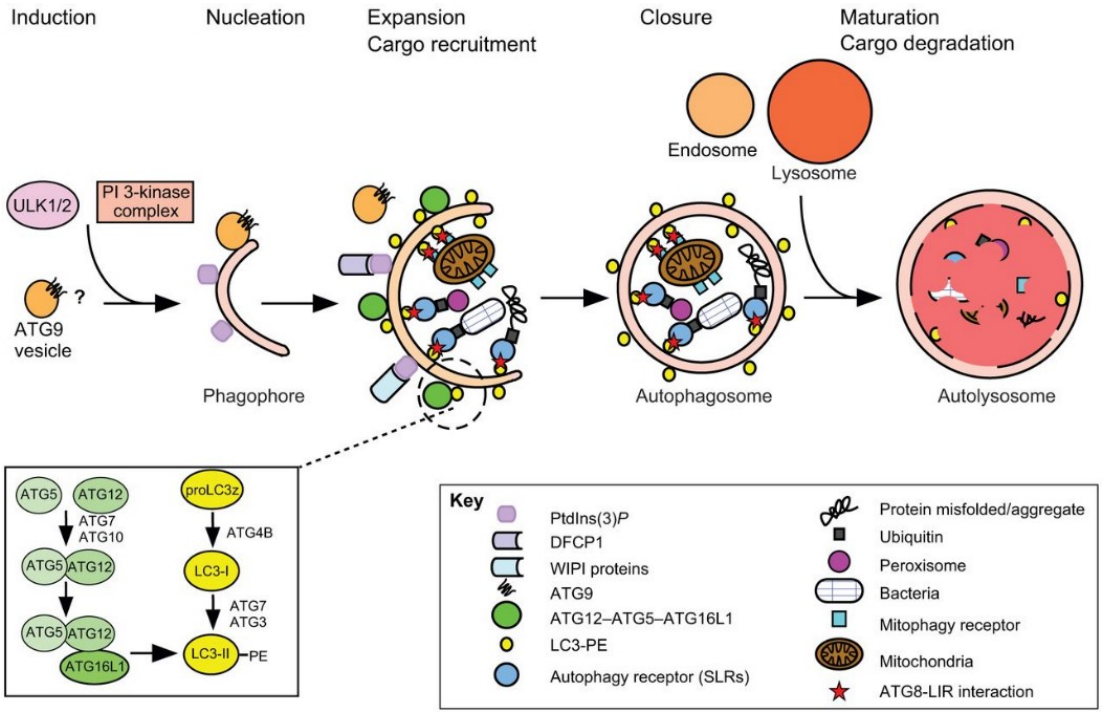

Figure 6. Overview of autophagy in mammalian cells.
Activation of the complex 51-like kinases 1 and 2 (ULK1/2) and specific scaffold proteins is essential for the induction of autophagy. During nucleation, proteins and lipids are recruited to the phagophore. The class III phosphatidylinositol 3-kinase (PI3-kinase) complex together with catalytic and regulatory subunits, like Beclin-1, induces the assembly of an autophagy compatible structure at the phagophore. Expansion of the phagophore depends on two ubiquitin-like (Ub) conjugation systems. LC3 proteins are conjugated to phosphatidylethanolamine (PE) and the exposure of a C-terminal glycine residue of proLC3 enables PE covalent attachment. Autophagic cargo is recruited to the inner growing phagophore by autophagy receptors and as the phagophore expands, a double-membrane autophagosome is formed. Autophagosome fusion with the lysosome forms the autolysosome and the cargo enclosed is degraded. From: Birgisdottir, Å. B. et al. (2013).

Considering that we are looking at a very complex mechanism, assessment and characterisation of autophagic flux provides important information to understand how autophagy is working. To achieve this, autophagy can be manipulated using inhibitors. Autophagosome-lysosome fusion can be blocked by Bafilomycin A1 (Baf A) that simultaneously blocks vacuolar ATPase pump activity present in the lysosome and disrupts the fusion between the autophagosome and the lysosome[58]. Another way to inhibit autophagy is by blocking lysosomal degradation with ammonium chloride that leads to acidification of the lysosome or with Leupeptin that inhibits lysosomal proteases.

1.6.2 Autophagy in atherosclerosis

In basal conditions, autophagy constitutes a major cytoprotective mechanism for both EC and SMC[59]. The ageing process is naturally accompanied with a decline in autophagy efficiency, which contributes to age-related endothelial dysfunction[46], leaving arteries more prone to plaque accumulation. Autophagy has a beneficial role in atherosclerosis, but in advanced stages of plaque accumulation, autophagy becomes dysfunctional and detrimental[60].

1.6.3 Autophagy in smooth muscle cells

Defective autophagy is very prejudicial and has been implicated in the particular case of SMC, because it triggers the development of CVD, namely atherosclerosis[61]. These cells have high percentage autophagic activity, which is also true in atherosclerotic plaques[62]. However, its impairment is associated with atherosclerosis progression[63]. Deficient autophagy affects SMC functionality and morphology and is responsible for the transition from a contractile phenotype to a synthetic and proliferative one[64], leading to postinjury neointima formation. Thus, a good approach to prevent ISR relies on a controlled stimulation of SMC autophagy[59]. Rapamycin is widely used as an autophagy inducer and antirestenotic agent[65] and sirolimus, the analogue of rapamycin, is nowadays the most common drug eluted in stents (SES).

1.6.4 Autophagy in endothelial cells

EC also benefit from basal autophagy, being a key cellular mechanism that ensures the preservation of its functions and CVD prevention[59]. However, when SES are implanted to prevent restenosis, sirolimus affect not only the SMC but also the EC.

1.6.4.1 Sirolimus-induced EC autophagy

The lining layer of EC that covers the tunica intima is what dictates artery wall health and thus, its integrity is crucial. As described above, stent inflation within the narrowed area leads to endothelium denudation and EC population decline.

Sirolimus, as a potent cytostatic agent, blocks cell cycle progression in SMC and EC, and as a mTOR inhibitor induces autophagy in both cell types. Autophagy induced by

sirolimus triggers very harmful phenotypic changes in EC. It impairs endothelium regeneration capacity and re-endotheliazation and consequently, arterial healing is delayed. Sirolimus-induced autophagy arrests the artery response towards endothelium regrowth and ultimately leads to endothelial dysfunction. Moreover, EC angiogenesis is also impaired since angiogenic potential is dependent on tissue integrity[66].

Considering that the endothelium is the gatekeeper of coronary artery health, its denudation together with the autophagy in those few EC that remain after stent inflation, predictably leads to ISR, after which myocardial infarction and death is just an odds game. Taking this into account, EC autophagy manipulation seems to be a good therapeutic approach to prevent ISR in patients with SES.

1.7 Statins

Statins are 3-hydroxy-3-methylglutaryl-CoA (HMG-CoA) reductase inhibitors routinely used in clinical practice to lower patients cholesterol levels and are widely prescribed as cardioprotective drugs[67]. In atherosclerosis, elevated blood cholesterol levels, or hypercholesterolemia, is a major risk factor to development and progression of this disease[68]. Statin intake is beneficial due to their capacity to inhibit the conversion of HMG-CoA into mevalonate, which is a precursor of cholesterol synthesis[69]. Therefore, cholesterol production by the liver is reduced and normal blood cholesterol levels are preserved[70].

1.7.1 Statins pleiotropic effects in SMC and EC

Surprisingly, HMG-CoA reductase inhibitors have shown to possess important pleiotropic effects like the activation of AMP-activated protein kinase (AMPK) pathway that leads to autophagy stimulation[54]. More importantly, clinical and experimental studies have described that statins, through autophagy activation, inhibit SMC proliferation and migration, like sirolimus. Several studies have reported that EC also benefit from statins pleiotropic effects. Its administration largely improves endothelial function, stabilizes atherosclerotic plaques and attenuates vascular remodelling and inflammation[67]. Statins also proved to hold protective effects ameliorating EC proliferation and migration, primarily impaired by sirolimus administration[71].

Interestingly, statins used in combination with PCI with stent implantation ware tested in patients with severe CAD. This conjugation was found to be safe and has shown significant synergistic effects and reduced ischemia and necrosis[72]. Nevertheless, a proper characterization of EC response to statins and sirolimus still needs to be investigated, thus leaving an open therapeutic window to study a different ISR treatment approach.

2. Objectives

The uninterrupted function of the heart is vital from embryogenesis and throughout life. The heart beats in a synchronized and coordinated manner and this capacity depends on the existence of intercellular channels, GJ. These display a crucial role in intercellular communication within blood vessels and insures the interaction between SMC and EC. These GJ are formed by connexins and disruption of GJ and changes in connexin expression levels have been associated with CVD development. Since Cx43 is the most abundantly expressed connexin in the heart and give important information about cell-cell communication, this protein has a relevant role in this study. Therefore, we intend to study the modulation of Cx43 protein expression levels.

Endothelial dysfunction is well described in the literature as a hallmark of atherosclerosis and it impairs EC intrinsic cellular processes like migration, proliferation and new vascular structures formation. Together, this impairment compromises proper recovery after tissue damage as found after stent opening, resulting in ISR. Despite SES represented a big step towards stenosis treatment, in 8 to 20% of the cases ISR continues to develop.

Several studies have described statins capacity to improve endothelial function, particularly ameliorating EC migration and proliferation capacity primely impaired by sirolimus administration. Therefore, being simvastatin the most prescribed statin among CVD patients, one of the main objectives of this study is to evaluate the effect of simvastatin in several EC functions, namely migration, proliferation and capillary-like structures formation *in vitro.*

Moreover, statins have proven able to inhibit SMC proliferation through autophagy activation like sirolimus. However, HMG-CoA reductase inhibitors effect in EC autophagy has not yet been well described. So, as a second main objective of this work we aim to evaluate simvastatin effect in EC autophagy modulation.

With this study we aim to assess if sirolimus and simvastatin possess a cooperative effect as a conjugated therapy to prevent ISR.

3. Materials and methods

3.1 Cell culture

3.1.1 Mouse cardiac endothelial cell line

The mouse cardiac endothelial cell line (MCEC-1) was developed by the Faculty of Medicine, National Heart & Lung Institute in London, United Kingdom and nobly provided by Professor Justin Mason[73]. The cell line was maintained in Dulbecco's Modified Eagle Medium (DMEM) (Life Technologies, Carlsbad, CA), supplemented with 10% fetal bovine serum (FBS), 1% Penicillin/Streptomycin (100 U/mL:100 µg/mL) and 1% GlutaMAX (Life Technologies, Carlsbad, CA), with 10 U/mL heparin (Sigma-Aldrich, St. Louis, MO) and 75 µg/mL endothelial cell growth factor (ECGF) (Sigma-Aldrich, St. Louis, MO, USA). MCEC-1 were cultured in 1% gelatin (Sigma-Aldrich, St. Louis, MO).

3.1.2 Human pulmonary arterial endothelial cells

The human pulmonary arterial endothelial cells (PAEC) were obtained from GIBCO (Life Technologies, Carlsbad, CA, USA). PAEC were cultured in Medium 200 (Life Technologies, Carlsbad, CA, USA) supplemented with 2% Low Serum Growth Supplement (LSGS) (Life Technologies, Carlsbad, CA, USA) and 1% Penicillin/Streptomycin (100 units/mL:100 µg/mL) (Life Technologies, Carlsbad, CA, USA). The cells were cultured in gelatin/fibronectin (0.02% gelatin/0.1% fibronectin) (Sigma-Aldrich, St. Louis, MO).

3.2 Isolation of porcine smooth muscle cells

Fresh porcine aortae, 10-14 cm in length, were sourced from 4 pigs. The aortae were rinsed with cold phosphate-buffered saline (PBS) (1.5 mM KH_2PO_4, 155 mM NaCl and 2.7 mM $Na_2HPO_4.7H_2O$ pH 7.4) and 1% Penicilin/Streptomycin/Amphotericin B (100 units/mL of penicillin, 100 µg/mL of streptomycin and 2.5 µg/mL of Amphotericin B) (Life Technologies, Carlsbad, CA) to remove all residual blood. Briefly, each aorta was cut open and placed in a petri dish with the tunica intima facing up, and any remaining endothelial cells were scraped. Then, tunica media and tunica adventitia were peeled off and separated. The tunica adventitia was discarded and the tunica media was cut into 2-3mm pieces, placed in a 20mm petri dish and incubated for 1.5 hours in 0.2% (w/v) collagenase type I (Life Technologies, Carlsbad, CA) in DMEM at 37°C. After this incubation, cell-enzyme solution was gently removed and discarded, and was replaced by 0.1% (w/v) collagenase type I in DMEM and tissue fragments were further incubated for 10 hours at 37°C. This step allows cells to dissociate from tissue segments. The collagenase solution was then deactivated with equal volume of Human Smooth Muscle Growth Media (Thermo Fisher Scientific) supplemented with 1% Low Serum Growth Supplement (Thermo Fisher Scientific), 5% FBS and 1% Penicillin/Streptomycin/Amphotericin B (100 units/mL of penicillin, 100 µg/mL of streptomycin and 2.5 µg/mL of Amphotericin B) (Life Technologies, Carlsbad, CA) and filtered through a 70-µm cell strainer to eliminate large pieces of aortic tissue. The collected cell suspension was centrifuged at 300g for 5 min at room temperature and the pellet was re-suspended and of then plated in Human Smooth Muscle Cell Growth Media at 37°C with 5% CO_2. The cell culture was not disturbed for 48 hr and after that media was completely removed and replaced with fresh media every second day.

All cells were maintained at 37°C with 5% CO_2, and cell plating was performed 24 to 48 hours prior to experimentation, unless otherwise indicated.

3.3 Cell treatments

3.3.1 Starvation

When indicated, starvation was induced in MCEC-1 by culturing cells in DMEM (Life Technologies, Carlsbad, CA), 1% antibiotics (100 U/ml penicillin, 100 µg/mL streptomycin) and 1% GlutaMAX (Life Technologies, Carlsbad, CA), not supplemented with FBS. Starvation was also induced in MCEC-1 by culturing cells in Hank's Balanced Salt Solution (HBSS) (5.3 mM KCl, 0.44 mM KH_2PO_4, 4.16 mM $NaHCO_3$, 137.9 mM NaCl, 0.38 mM Na_2HPO_4 and 5.5 mM D-Glucose) with calcium and magnesium.

3.3.2 mTOR and autophagy inhibitors

When indicated, cells were treated with different inhibitors: mammalian target of rapamycin (mTOR) inhibition was induced by the addition of 50 nM Rapamycin (Tocris Bioscience, Bristol, UK); lysosome-dependent degradation was inhibited by the addition of 100 nM Bafilomycin A1 (Baf) (Millipore, Bedford, MA, USA); or 20 mM Ammonium chloride (NH_4Cl) (Sigma Aldrich, St. Louis, MO, USA) plus 100 µM Leupeptin (Leup) (Sigma Aldrich, St. Louis, MO, USA).

3.3.3 Simvastatin

Cells were also treated with 1 µM, 5 µM and 10 µM of activated Simvastatin (Sigma Aldrich, St. Louis, MO, USA). To cell culture use, Simvastatin needs to be activated by opening of the lactone ring. Briefly, Simvastatin (0.019 mM) was dissolved in 100% ethanol, with subsequent addition of 0.1 N NaOH until a final volume of 0.5 mL. The solution was heated at 50°C for 2 hours in a sand bath and then neutralized with HCl (pH 7.2) before being brought to a final volume of 1 mL with distilled water. Activated Simvastatin was stored at −80°C until use.

3.4 MTT cell viability assay

To evaluate MCEC-1 and PAEC metabolic activity after treatments, cells were seeded onto 24-well plates and, after the indicated treatments, washed twice with PBS and incubated with 0.5 mg/mL MTT [3-(4,5-dimethylthiazol-2-yl)-2,5-diphenyltetrazolium bromide; Invitrogen, Carlsbad, CA, USA] in DMEM for 1.5 hours in a cell culture incubator at 37°C with 5% CO_2. Subsequently, supernatants were removed and the precipitated dye was dissolved in 300 µL 0.04 M HCl (in isopropanol). Absorbance readings of the dissolved formazan crystals were performed at a wavelength of 570 nm, with wavelength correction at 620 nm, using a Biotek Synergy HT spectrophotometer (Biotek, Winooski, VT, USA).

3.5 Western blot (WB) analysis

After appropriate treatments, cells were washed twice in ice-cold PBS, scraped in RIPA buffer (150 mM NaCl, 50 mM Tris-HCl, 1% NP-40 and 0.1% SDS, pH 7.5), containing protease and phosphatase inhibitors. Cell lysates were incubated for 30min on ice, and the solubilized fraction was recovered in the supernatant after centrifugation at 12000 g for 10 min, at 4°C. Protein supernatants were denatured with 2x Laemmli buffer (125 mM Tris, pH 6.8, 4% [weight/volume] SDS, 20% [volume/volume] glycerol, 10% [volume/volume] ß-mercaptoethanol, 0.006% bromophenol blue) and heated at 95°C for 5 min.

When indicated, cells were washed twice in ice-cold PBS, and scraped in 2x Laemmli buffer and denaturated at 95°C for 5 minutes.

Total cell lysates were separated by sodium dodecyl sulfate polyacrylamide gel electrophoresis (SDS-PAGE), and transferred to nitrocellulose membranes (Bio-Rad Laboratories, Hercules, CA, USA). The membranes were blocked with 5% [weight/volume] non-fat milk in Tris-buffered saline-Tween 20 (TBS-T) (20mM Tris, 150 mM NaCl, 0.2% Tween 20, pH=7.6), probed with appropriate primary antibodies and horseradish peroxidase (HRP)-conjugated secondary antibodies. All antibodies used in this method are listed in Table 1. The proteins of interest were visualized by chemiluminescence using Clarity™ western ECL substrate (Bio-Rad Laboratories, CA, USA) according to the manufacturer's instructions. The chemiluminescent blots were imaged on ImageQuant™ LAS 500 (GE Healthcare Life Sciences, Piscataway, NJ, USA).

Densitometric quantification was performed in unsaturated images using ImageJ (National Institutes of Health, Bethesda, MD).

3.6 Immunofluorescence staining

Cells grown on glass coverslips were fixed with 4% paraformaldehyde (PFA) in PBS for 10 minutes. The samples were then washed three times with PBS, permeabilized with 0.2% v/v Triton X-100 in PBS, for 10 minutes and blocked with 2.5% Bovine Serum Albumin (BSA) for 20 minutes. Incubation with primary antibodies proceeded overnight in a humid chamber at 4°C. The samples were then washed three times with PBS before incubation with the secondary antibody for 1h at room temperature. Nuclei were stained with DAPI. The specimens were rinsed in PBS and mounted with Mowiol 4-88 Reagent (Calbiochem, San Diego, CA). All antibodies were diluted in 2% w/v BSA in PBS. The control immunostaining specificity was performed by omitting the primary antibodies. All antibodies used in this method are listed in Table 1. The images were collected by fluorescence microscopy using a Zeiss Axio HXP IRE 2 (Carl Zeiss AG, Jena, Germany).

3.7 Ki67 proliferation assay

Proliferation rates of EC was assessed using the nuclear protein Ki67 as a cell proliferation-associated marker. After 24 hours of treatment, cells grown on glass coverslips were fixed, permeabilized, blocked, immunostained and mounted as described above. Cells were stained with DAPI (staining the nuclei) and with Ki67 (staining proliferating cells). Proliferation rates was calculated as the ratio between the number of cells positively stained for Ki67 and the number of cells stained for DAPI.

3.8 Wound healing assay

The wound healing assay was employed to measure MCEC-1 and PAEC migration. After 24 hours of treatment, EC migration was assessed by scratching a confluent layer of cells in the centre of a 12-well plate using the extremity of a 20 to 200 µL sterile pipette tip. Detached cells were removed by a PBS wash and 1 mL of medium was added, followed by incubation at 37°C in 5% CO_2. Phase contrast images were taken immediately after the scratch and 2, 4, 6 and 8 hours later using a Zeiss Axio HXP IRE 2 microscope (Carl Zeiss AG, Jena, Germany). The reduction of wound area was quantified using ImageJ.

3.9 Matrigel angiogenesis assay

The angiogenic potential of MCEC-1 and PAEC cells was tested using the Matrigel angiogenesis assay. In the day before experimentation, the lower well of the µ-Slide Angiogenesis (Ibidi, Martinsried, Germany), containing or not in the well a piece of Bare-metal stent (Tsunami® Gold, TERUMO, Tokyo, Japan) or Sirolimus-eluting stent (Ultimaster™, TERUMO, Tokyo, Japan), was filled with 10 µL of Matrigel (Corning® Matrigel® Matrix Growth Factor Reduced, BD Biosciences, Fairleigh, NJ, USA). After matrigel polymerization, for 30 minutes at 37°C, 20 µL of cell culture medium was added to each well and the µ-Slide Angiogenesis was left overnight at 37°C in a humidity chamber to prevent matrigel drying. Then, MCEC-1 or PAEC were seeded, in a total volume of 50 µL of medium, with or without treatments onto the solidified Matrigel. Phase-contrast images were collected 8 hours after MCEC-1 seeding and 6 hours after PAEC seeding, using Zeiss Axio HXP IRE 2 microscope (Carl Zeiss AG, Jena, Germany). The images were analysed using the plugin of angiogenesis for ImageJ (National Institute of Health, Bethesda, MD, USA).

3.10 Statistical analysis

All data are representative of at least three independent experiments. Results were analysed with GraphPad Prism 6 for Windows, version 6.01 (GraphPad Software, Inc.) and are expressed as mean ± S.D. Two-way ANOVA with Tukey multiple comparisons test was applied. Differences were considered significant at $p<0.05$.

Table 1. List of primary and secondary antibodies used for the Western Blot and Immunofluorescence.

Antibody	Host/Clonality	Clone/Cat#	Application	Dilution	Company
anti-Cx43	goat polyclonal	AB0016-500	WB/IF	1:5000/1:200	SICGEN (Cantanhede, Portugal)
anti-Cx43	mouse monoclonal	610062	IF	1:25	BD Transduction Laboratories (CA, USA)
anti-LC3	rabbit polyclonal	PA1-16931	WB/IF	1:1000/1:100	Thermo Fisher Scientific, Carlsbad, CA, USA
anti-p62/SQSTM1	rabbit polyclonal	5114s	WB	1:1000	Cell Signaling Technology, Beverly, MA, USA
anti-Beclin 1	rabbit polyclonal	B6186	WB	1:500	Sigma-Aldrich (St. Louis, MO, USA)
anti-p-mTOR	rabbit polyclonal	2971	WB	1:1000	Cell Signaling Technology, Beverly, MA, USA
anti-Calnexin	goat polyclonal	AB0041	WB	1:5000	SICGEN (Cantanhede, Portugal)
anti-GAPDH	goat polyclonal	AB0049	WB	1:5000	SICGEN (Cantanhede, Portugal)
anti-Ki67	mouse monoclonal	Sc-23900	IF	1:100	Santa Cruz Biotechnology (Heidelberg, Germany)
anti-αSMA	mouse monoclonal	A5228	IF	1:2000	Sigma-Aldrich (St. Louis, MO, USA)
anti-goat-HRP	rabbit	61-1620	WB	1:10000	BioRad (Hercules, CA, USA)
anti-rabbit-HRP	goat	656120#	WB	1:10000	Life Technologies (Carlsbad, CA)

alexa 488 anti-goat	donkey/IgG	A11055	IF	1:500	Molecular Probes, Life Technologies (Carlsbad, CA)
alexa 488 anti-mouse	goat/IgG	A11001	IF	1:500	Molecular Probes, Life Technologies (Carlsbad, CA)
alexa 568 anti-rabbit	goat/IgG	A11011	IF	1:500	Invitrogen, Life Technologies (Carlsbad, CA)
alexa 594 anti-mouse	donkey/IgG	R37115	IF	1:500	Molecular Probes, Life Technologies (Carlsbad, CA)

4. Results

4.1 Metabolic activity of both MCEC-1 and PAEC is not affected by rapamycin and simvastatin treatment

Before starting this work, we needed to ensure that the treatments we intended to subject cells to would not affect their metabolic activity and, consequently, cellular viability. For this purpose, we performed MTT assays in MCEC-1 and PAEC.

Briefly, two different types of endothelial cells, MCEC-1 and PAEC were incubated for 24 hours with 50 nM Rapamycin, three different concentrations of Simvastatin, namely 1, 5 and 10 µM and with a combination of 50 nM Rapamycin and 1 µM Simvastatin. In the case of MCEC-1, the metabolic activity was additionally evaluated either in the presence or absence of a lysosome inhibitor. For this, cells were incubated for 24 hours with 1 µM Simvastatin with an incubation of 100 nM Bafilomycin A1 in the last 6 hours of treatment.

Metabolic activity in both MCEC-1 and PAEC do not seem to be affected by our experimental conditions, as demonstrated in Figure 7A and Figure 7B respectively.

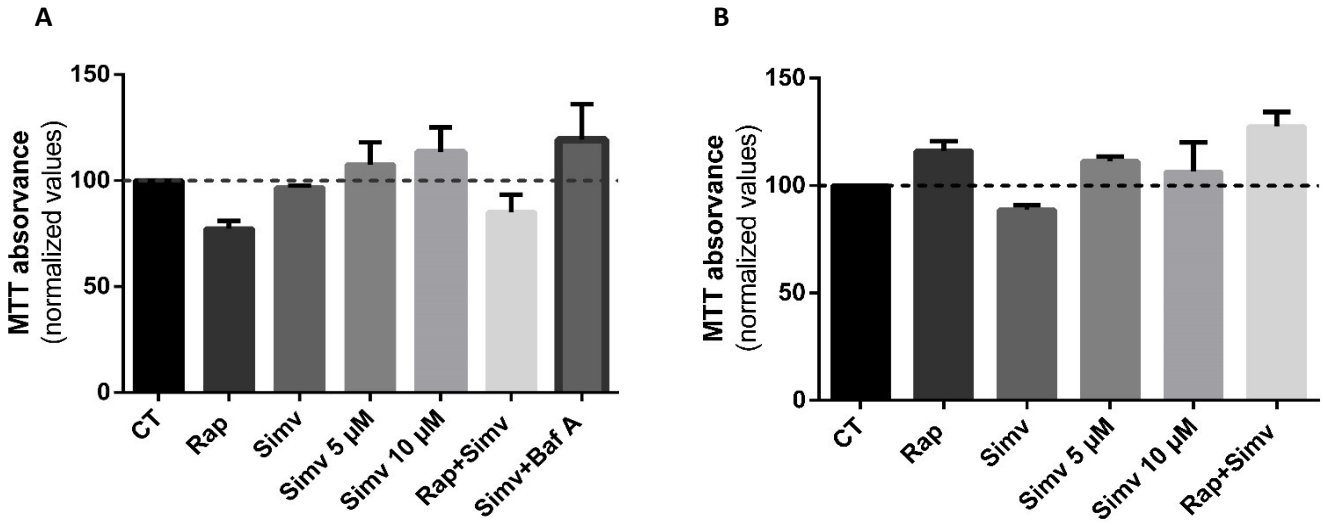

Figure 7. Metabolic activity of MCEC-1 and PAEC in response to rapamycin and simvastatin treatment.
MCEC-1 and PAEC cellular viability was evaluated by MTT assay after being subjected to the indicated treatments for 24 hours. Where indicated, 100 nM of Bafilomycin A1 was added in the last 6 hours of treatment. (A) Representative graph showing normalized values of MTT absorbance in MCEC-1. (B) Representative graph showing normalized values of MTT absorbance in PAEC. Results represent mean ± S.D. of triplicate samples from two independent experiments in both MCEC-1 and PAEC.

4.2 Effect of rapamycin and simvastatin treatment in EC migration

Endothelial dysfunction is associated with diminished capacity of EC to form new vascular structures which affects cellular processes like cell migration[11]. Experimental studies have already described that statins can inhibit SMC migration[67]. Interestingly, also in EC, statins have shown beneficial pleiotropic effects, for instance ameliorating EC migration primarily impaired by sirolimus administration[67].

To evaluate whether statins can modulate migration in the EC studied in this work, we started by investigating the separately effect of rapamycin and simvastatin, which is the most common statin prescribed to treat hypercholesterolemia, and the co-treatment of rapamycin and simvastatin. With that purpose, we used a scratch assay in which cell migration into the wound space was quantified.

4.2.1 Conjugation of rapamycin with simvastatin attenuates simvastatin-induced migration retardation in MCEC-1

The results presented in Figure 8, demonstrate that MCEC-1 incubated with 50 nM Rapamycin (hereafter referred to as rapamycin), which corresponds to the average rapamycin concentration found in the blood circulation of patients with SES implanted, induce cells to migrate more than those incubated with 1 µM Simvastatin (hereafter referred to as simvastatin), which corresponds to the average simvastatin concentration found in the blood circulation of patients after oral administration. Nevertheless, the combined treatment of 50 nM Rapamycin and 1 µM Simvastatin (hereafter referred to as Rap+Simv) seems to attenuate simvastatin-induced migration retardation. Higher concentrations of simvastatin, namely 5 and 10 µM, delays MCEC-1 migration. Representative phase-contrast images obtained immediately after the scratch and 24 hours after are shown in Figure 8A.

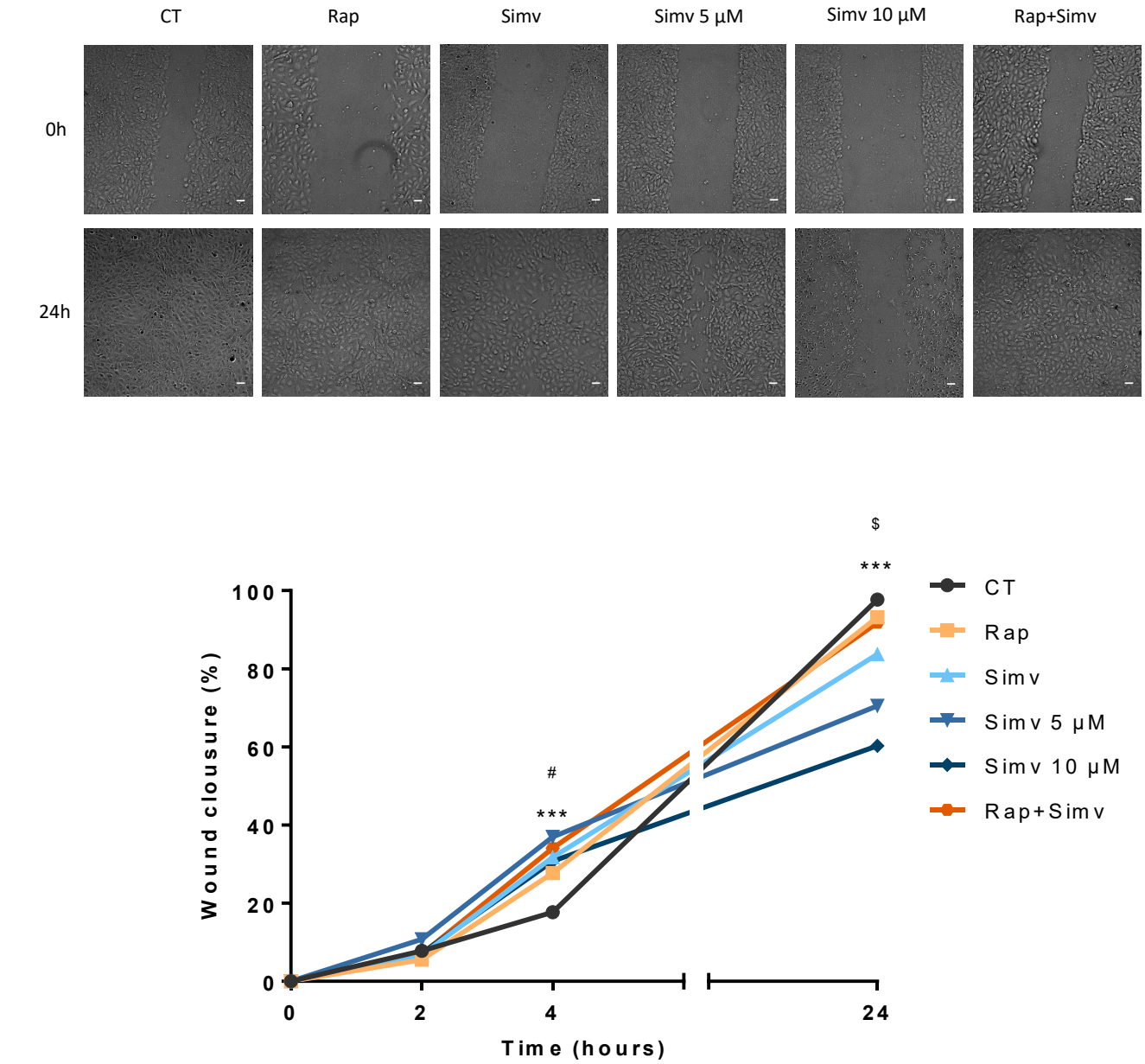

Figure 8. Combined treatment of rapamycin and simvastatin attenuates simvastatin-induced migration retardation in MCEC-1.

Migration capacity of MCEC-1 was assessed through wound healing assays. MCEC-1 were treated for 24 hours after which, the confluent monolayer was scratched and cell migration was monitored for 24 hours. (A) Representative phase-contrast images at time 0 (immediately after the scratch) and 24 hours after the scratch. Scale bars 100 µm. (B) Quantification was performed in images taken at the beginning of the assay and at the indicated times after the scratch. Cell-free area was measured using ImageJ. Results represent the mean ± S.D. wound size area of triplicate samples from four independent experiments. ***p<0.001 CT vs Simv, #p<0.05 CT vs Rap, $p<0.05 Rap vs Simv.

4.2.2 Higher concentrations of simvastatin ameliorate PAEC migration capacity

After testing migration capacity in an endothelial cell line (MCEC-1), we evaluated the same parameter and the same experimental conditions in primary endothelial cells, PAEC. Results presented in Figure 9 show that 5 μM Simvastatin and rapamycin alone are more efficient in inducing PAEC migration, while 1 μM Simvastatin delays PAEC migration. These results are consistent with the wound healing response in MCEC-1, with the same tendency of 1 μM Simvastatin to retard EC migration compared with rapamycin. Contrarily to MCEC-1, in PAEC rapamycin did not affect the simvastatin-induced decrease of cell migration. Representative phase-contrast images presented in Figure 9A were obtained at time 0 and 8 hours after the scratch.

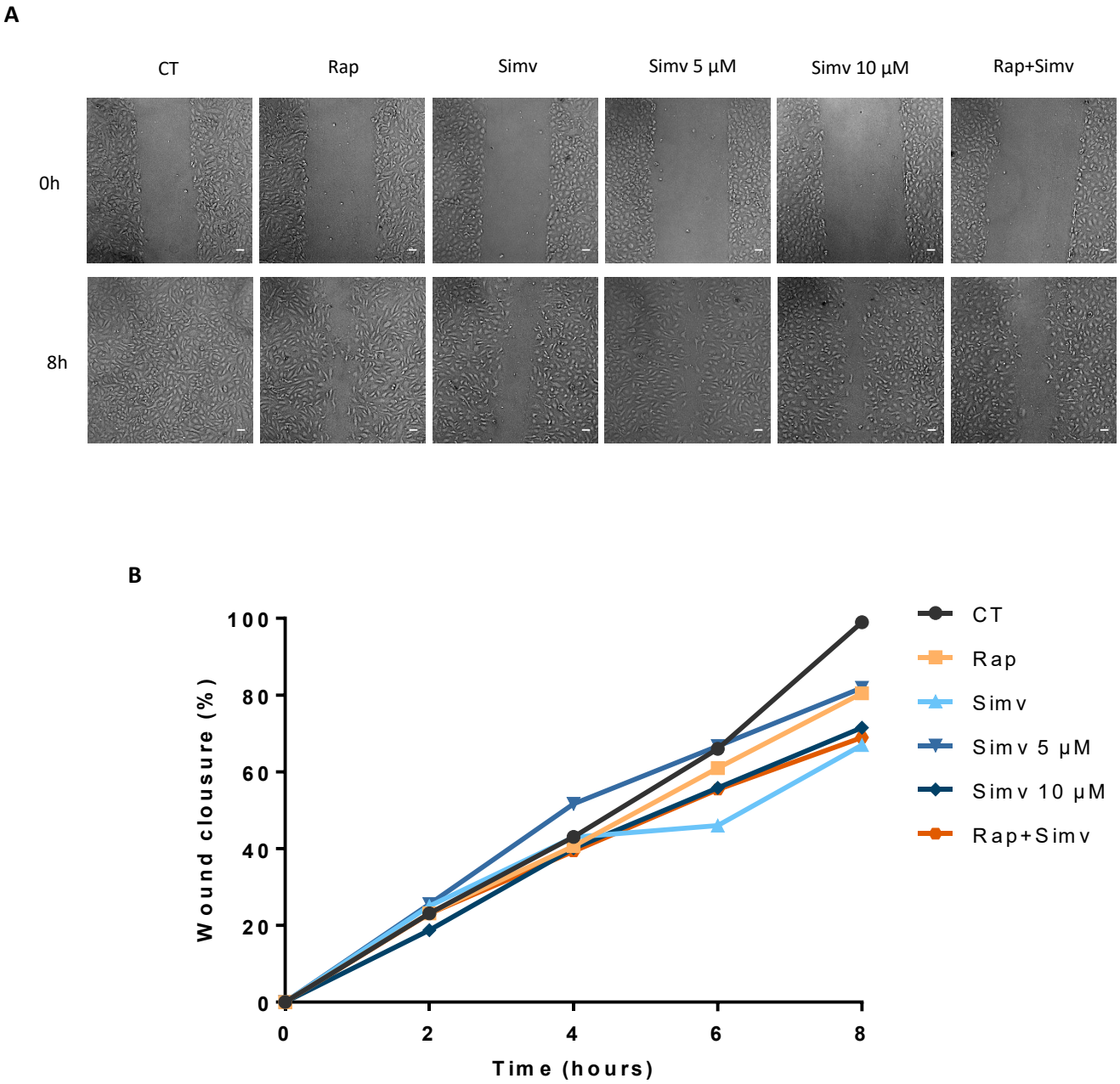

Figure 9. Higher concentrations of Simvastatin ameliorate PAEC migration capacity.
Migration capacity of PAEC was assessed by wound healing assays. PAEC were incubated with the indicated experimental conditions for 24 hours, after which the confluent monolayer was scratched and cell migration was monitored for a period of 8 hours. (A) Representative phase-contrast images at time 0 (immediately after the scratch) and 8 hours after the scratch are shown. Scale bars 100 µm. (B) Quantification was performed in the images taken at the beginning of the assay and at the indicated times after the scratch. Cell-free area was measured, using ImageJ. Results represent the mean ± S.D. wound size area of triplicate samples from two independent experiments.

4.3 Combined treatment of rapamycin and simvastatin in EC proliferation rates

It is well established that senescent endothelial cells have diminished proliferative capacity and have been implicated in endothelial dysfunction[47]. Evidence found in the literature describes that some statins have the capacity to induce proliferation in EC[71]. With this in mind, we pursued to validate this effect in our experimental model, with the endothelial cell line, MCEC-1, and primary cell cultures, PAEC.

To test whether rapamycin conjugated with simvastatin can have an effect in EC proliferation, both EC were incubated with 50 nM Rapamycin, three different concentrations of Simvastatin, namely 1, 5 and 10 µM, and a conjugation of 50 nM Rapamycin with 1 µM Simvastatin (Rap+Simv). Proliferation rates were assessed after 24 hours of treatment.

Ki67 is a nuclear protein expressed in all phases of the cell cycle except in the resting phase (G0) and for this reason is widely used as a marker of proliferation. The presence of Ki67 in our experimental conditions was evaluated by immunofluorescence.

4.3.1 MCEC-1 proliferation rates are not altered in response to rapamycin and simvastatin treatment

Figure 10A depicts representative immunofluorescence images from Ki67 staining in MCEC-1 after treatment.

The number of cells positively stained for Ki67 do not vary significantly throughout our experimental conditions as seen in Figure 10B. Nevertheless, there is a tendency for rapamycin to increase MCEC-1 proliferation and simvastatin to impair it. This impairment is more notorious under higher concentrations of simvastatin.

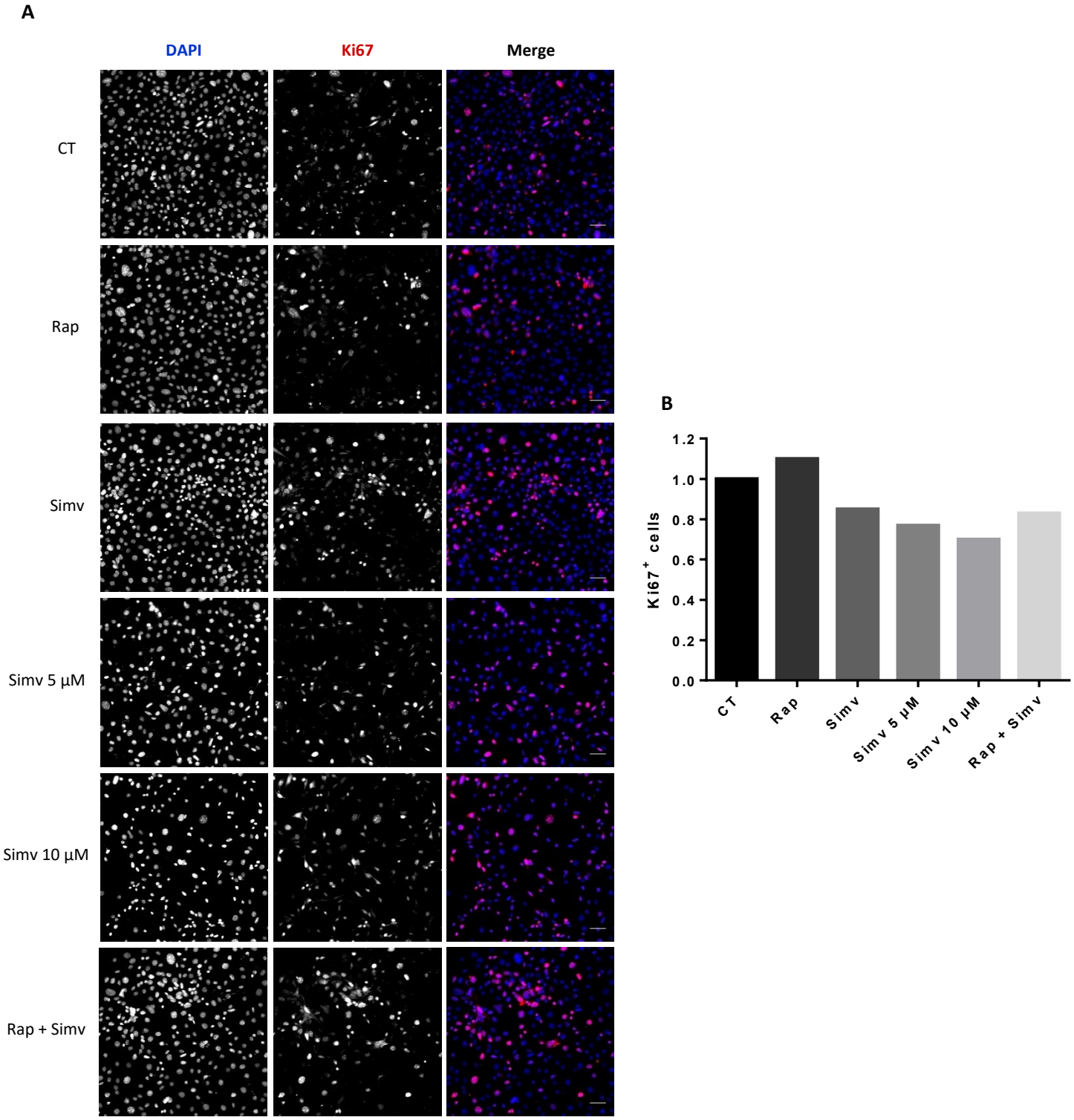

Figure 10. **Proliferation rates of MCEC-1 in response to rapamycin and simvastatin treatment.**
MCEC-1 were incubated for 24 hours with 50 nM Rapamycin, 1, 5 and 10 µM Simvastatin, or with 50 nM Rapamycin plus 1 µM Simvastatin. (A) Representative immunofluorescence images show cells positively stained for Ki67. Nuclei were stained with DAPI. (B) Quantitative assessment of proliferation rates was calculated as the ratio between the number of cells positively stained for Ki67 and the number of cells stained for DAPI. DAPI and Ki67 positive cells were quantified using ImageJ. Scale bars 50 µm. Data from one experiment (quantification of 15 images per condition).

4.3.2 Simvastatin and co-treatment of simvastatin with rapamycin impairs PAEC proliferation capacity

Representative immunofluorescence images from Ki67 staining in PAEC are shown in Figure 11A.

The number of Ki67 positively stained cells increases with rapamycin treatment, however this effect is prevented when cells are co-treated with simvastatin. Simvastatin treatment alone also decreases Ki67 staining in PAEC when compared to controls, as demonstrated in Figure 11B.

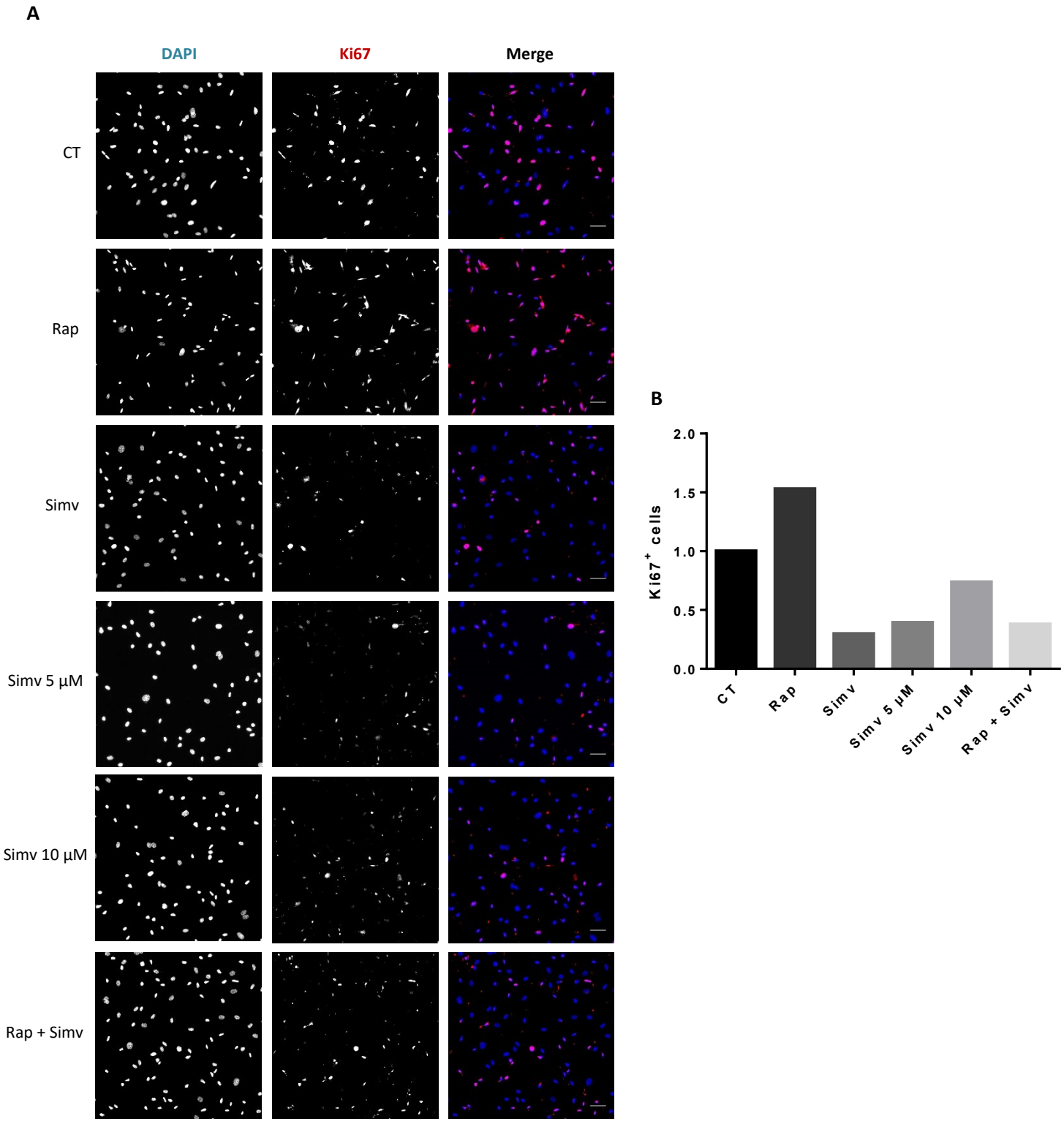

Figure 11. Proliferation rates of PAEC in response to rapamycin and simvastatin treatment.
PAEC were incubated for 24 hours with 50 nM Rapamycin, 1, 5 and 10 µM Simvastatin, or with 50 nM Rapamycin plus 1 µM Simvastatin. (A) Representative immunofluorescence images show cells positively stained for Ki67. Nuclei were stained with DAPI. (B) Quantitative assessment of proliferation rates was calculated as the ratio between the number of cells positively stained for Ki67 and the number of cells stained for DAPI. Nuclei stained with DAPI were quantified using ImageJ and cells positively stained for Ki67 were manually counted. Scale bars 50 µm. Data from one experiment (quantification of 15 images per condition).

4.4. Assessment of EC angiogenic potential

The capacity of EC to form new vascular structures is one of the intrinsic functions of this cell type. It is known that under endothelial dysfunction, their angiogenic capacity is compromised[14], which further impairs recovery after tissue damage[66]. With this in mind, we investigated the angiogenic response of MCEC-1 and PAEC under different treatments.

4.4.1. Simvastatin promotes angiogenesis *in vitro* and also reverts rapamycin-induced impairment of tube formation in MCEC-1

We assessed the basal capacity of MCEC-1 to form tubes as a measure of *in vitro* angiogenesis and then compared it to conditions in which rapamycin alone (Rap), simvastatin alone (Simv) or both (Rap+Simv) were added to the matrigel. To assess the direct effect of the stent on EC behaviour, in parallel, we also entrapped a piece of stent, either BMS or a SES, within the matrigel. In the case of SES, the matrigel with the embedded stent was incubated either in the presence (SES+Simv) or absence of simvastatin (SES). As a control to SES conditions, a piece of BMS alone (BMS) or a piece of BMS with simvastatin (BMS+Simv) was incubated within the matrigel (Table 2). Figure 12A shows representative phase-contrast images for each condition after 8 hours of MCEC-1 seeding.

As observed in Figure 12B, in the absence of the stent, rapamycin directly added to the medium seems to impair tube formation in MCEC-1 whereas simvastatin increases it. Indeed, Simv is able to increase all parameters analysed regarding tube formation, namely number of nodes, total master segments length and number of meshes. Importantly, the rapamycin-induced impairment of tubulation is reverted when simvastatin is added. Interestingly, as demonstrated in Figure 12C, the same tendency is observed in cells incubated in the presence of BMS or SES.

Table 2. Experimental conditions used in matrigel angiogenesis assay in MCEC-1. CT: no treatment added.

Matrigel	CT	CT	CT	CT	BMS	BMS	SES	SES
Condition	CT	Simv	Rap	Simv+Rap	CT	Simv	CT	Simv

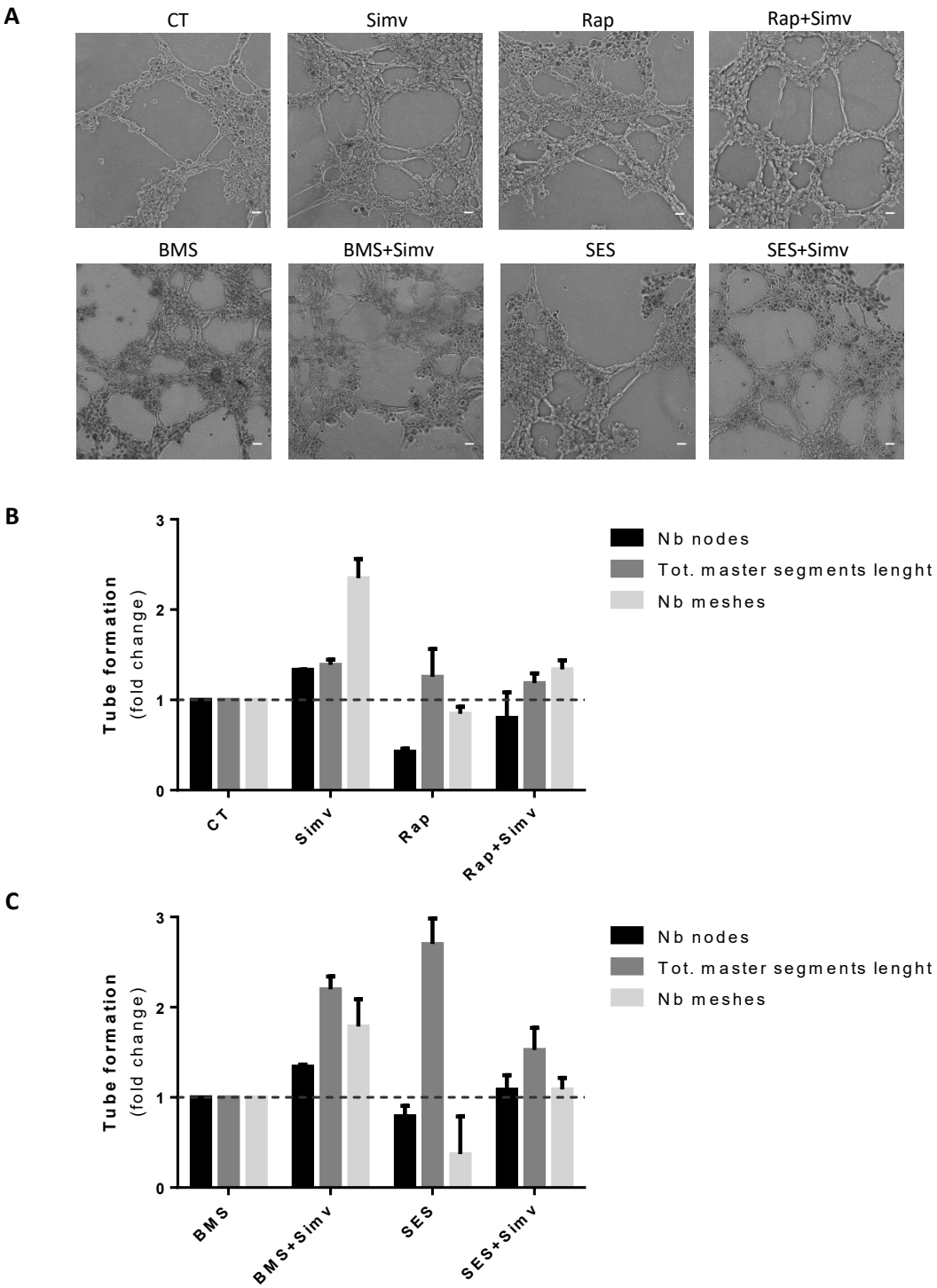

Figure 12. Simvastatin promotes MCEC-1 capillary-like structures formation *in vitro* and also counters the effect of rapamycin.

Capillary-like tube formation in matrigel assays was assessed 8 hours after MCEC-1 seeding with different treatments. (A) Representative phase-contrast images are shown. Scale bar:100 µm. Quantitative assessment of the number of meshes, nodes and total master segment length performed in conditions (B) without stent entrapped within the matrigel with results normalized to cells seeded with no treatments, and (C) in BMS and SES conditions with results were normalized to cells seeded in the presence of BMS alone. Results represent mean ± S.D. of triplicate samples from two independent experiments.

4.4.2. PAEC capillary-like structure formation *in vitro* is not regulated by simvastatin

We proceeded to test the angiogenic response to our treatments in the primary endothelial cell culture (PAEC). Thus, the method applied in PAEC was the same has above described, except for the presence of BMS conditions. In this case, we only used we only used the SES (Table 3). Figure 13A depicts representative phase-contrast images from each condition after 6 hours of PAEC seeding.

The results presented in Figure 13B shows a tendency for rapamycin to inhibit tubulation, but contrarily to MCEC-1, this effect was not reverted by simvastatin co-treatment (Rap+Simv). This result was corroborated when PAEC were incubated in a matrigel containing SES where the number of meshes, nodes and total master segments length do not seem to be affected by simvastatin addition, as showed in Figure 13C.

Table 3. Experimental conditions used in matrigel angiogenesis assay in PAEC. CT: no treatment added.

Matrigel	CT	CT	CT	CT	SES	SES
Condition	CT	Simv	Rap	Simv+Rap	CT	Simv

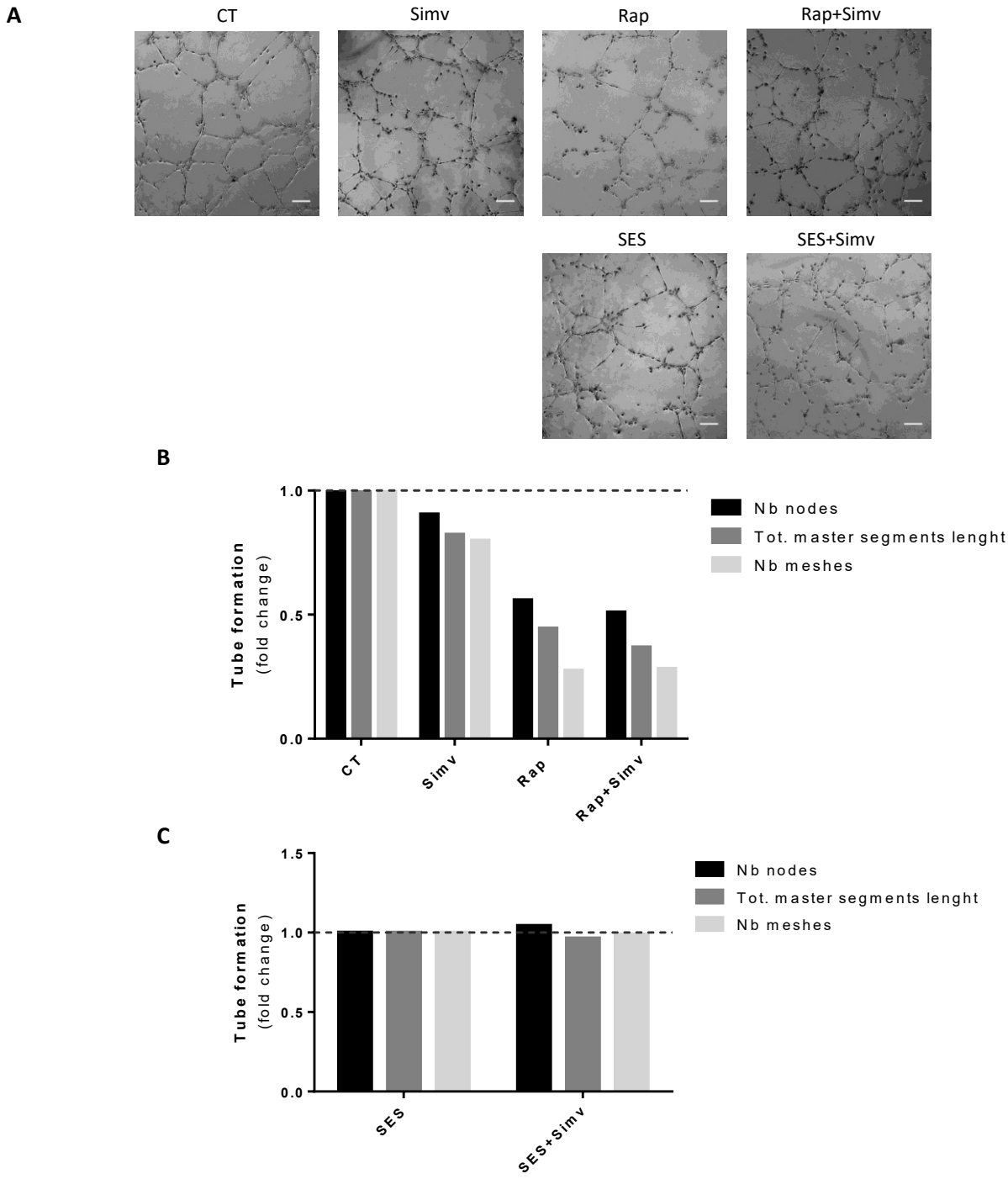

Figure 13 PAEC in *vitro* angiogenesis is not regulated by rapamycin.
Tube formation matrigel assays were assessed 6 hours after PAEC seeding with the described treatments. (A) Representative phase-contrast images are shown. Scale bars 100 µm. Quantitative assessment of the number of meshes, nodes and total master segment length (B) in conditions without a stent entrapped within the matrigel with results normalized to cells seeded with no treatments and (C) in SES conditions. ImageJ Pro Plus 5.1. was used to quantify the parameters. Results represent mean ± S.D. of triplicate samples from one independent experiment.

4.5. Characterization of autophagy in the mouse cardiac endothelial cell line MCEC-1

Considering that autophagy constitutes a very complex mechanism, different cell lines may respond differently to the same stimuli. Thus, the characterisation of basal autophagic flux is important in MCEC-1 is important to ensure that possible changes in autophagic response were due to the treatments applied.

To characterize the autophagy profile in this endothelial cell line, autophagy was manipulated using well established inducers and inhibitors, and the expression levels of proteins associated with the pathway were analysed by WB (Figure 14). To activate autophagy, we used 50 nM Rapamycin (Rap), a well known mTOR inhibitor, and starvation (ST), by culturing cells in medium without serum or HBSS that induces a more severe starvation. These last two autophagy activators, starvation and HBSS, are known to indirectly inhibit mTOR. Moreover, to prevent lysosomal protein degradation, we blocked autophagosome-lysosome fusion with 100 nM Bafilomycin A1 (Baf A), whereas lysosomal degradation was inhibited with 20 mM Ammonium chloride (NH_4Cl) or 100 µM Leupeptin (Leup).

Results presented in Figure 14B demonstrate that rapamycin, starvation and HBSS are efficiently inhibiting mTOR as demonstrated by the lower levels of p-mTOR when compared to control conditions or cells incubated with Baf A or NH_4Cl+Leup.

Accordingly, with mTOR inhibition and autophagy activation, as shown in Figure 14C, the levels of the autophagy receptor p62 decrease due to its lysosomal degradation in cells incubated in starvation, rapamycin or HBSS. In the presence of Baf A or NH_4Cl+Leup this degradation is prevented with an increase in p62 levels.

As demonstrated in Figure 14D, Rapamycin and HBSS also seem to decrease LC3-II levels, concordantly with p62. On the other hand, the levels of LC3-II are shown to slightly increase when MCEC-1 are incubated in starvation conditions, likely due to the conversion of LC3-I to LC3-II, which is involved in the formation of autophagic vesicles. Since at least part of this LC3-II is degraded after the fusion of the autophagosome with the lysosome, in the Baf A or NH_4Cl+Leup conditions the levels of LC3-II are increased due to lysosomal degradation impairment.

In Figure 14C and Figure 14D respectively, we show decreased expression levels of proteins associated with autophagy activation, namely p62 and LC3-II. In order to

strengthen these results, we investigated the impact of autophagy modulators upon the levels of a well-established autophagy substrate, Cx43, known to be vital for endothelial function. The results obtained show that Cx43 levels are also decreased in these conditions which suggests that Cx43 may be a substrate of autophagy in MCEC-1, as demonstrated in Figure 14E. Contrary to autophagy inducer conditions, as expected, the autophagy inhibitors Baf A and NH_4Cl+Leup led to an increase in p62, LC3-II and Cx43 protein levels.

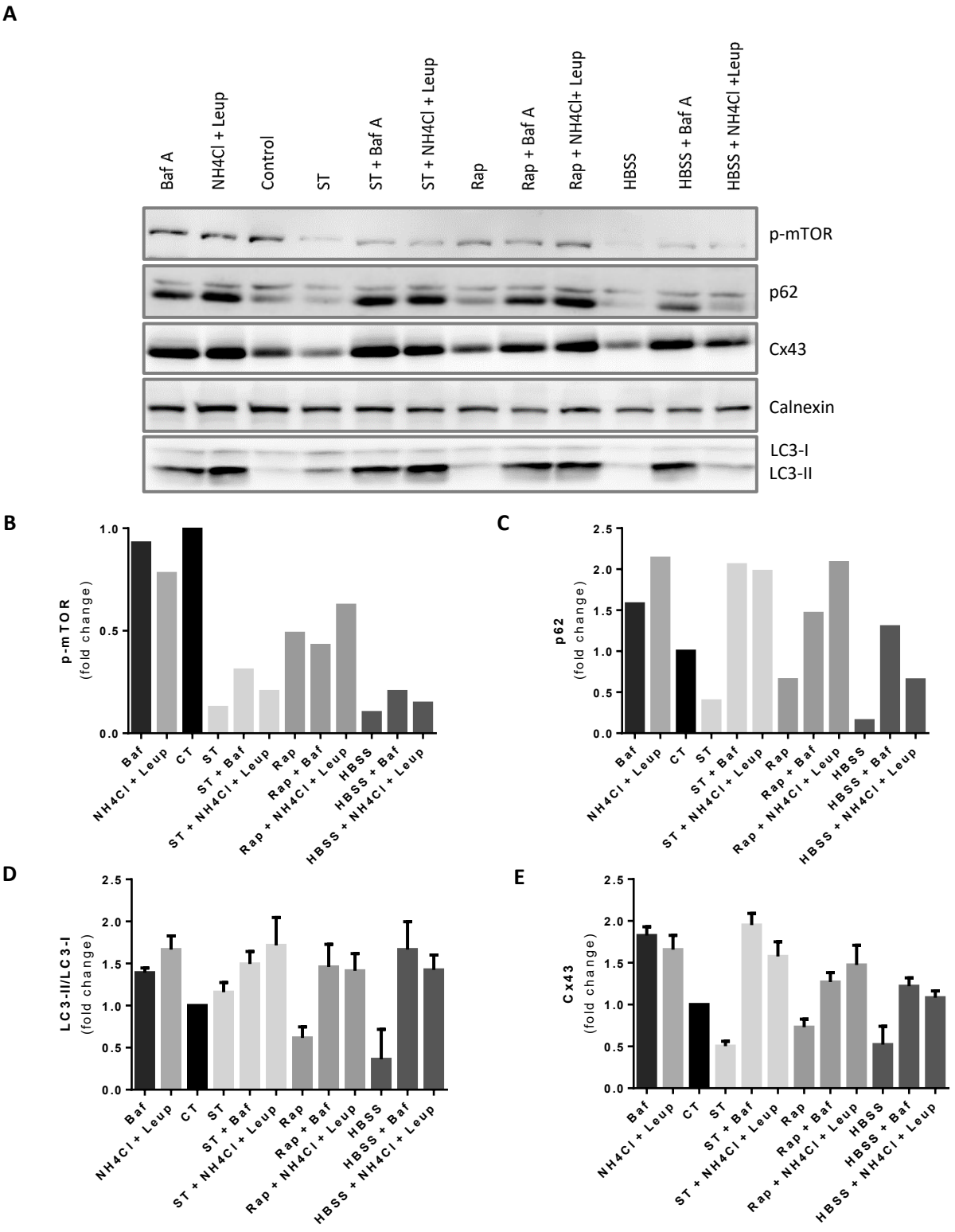

Figure 14. Expression levels of proteins associated with autophagy in MCEC-1 cells.
Expression levels of proteins implicated in the autophagy pathway were assessed by WB analysis after MCEC-1 were subjected for 24 hours to the indicated treatments. (A) Representative WB showing expression levels of p-mTOR, p62, Cx43 and LC3-II and LC3-I upon different conditions. Quantification of p-mTOR (B), p62 (C), LC3-II/LC3-I (D) and Cx43 (E) protein levels. Quantification of p-mTOR, p62 and Cx43 was normalized to Calnexin. Results represent mean ± S.D. of triplicate samples from one independent experiment in the case of p-mTOR and p62 and two independent experiments in the case of Cx43 and LC3-II/LC3-I.

4.5.1. Starvation and rapamycin induce autophagic vesicle formation

A common method to evaluate autophagy activation is the detection of LC3 containing vesicles in the cytoplasm of cells. Thus, in a subsequent stage of this work, we proceeded to confirm whether Cx43 is a substrate of autophagy in MCEC-1. To tackle this question, MCEC-1 were incubated with rapamycin or starvation conditions for 24 hours and autophagy activation was evaluated by immunofluorescence microscopy to detect LC3 puncta.

The results presented in Figure 15 demonstrate that starvation and rapamycin induce LC3 accumulation in a puncta pattern, corresponding to autophagic vesicle formation, suggesting that autophagy is being activated. Immunofluorescence images are concordant with the previous WB analysis, where starvation induces a greater accumulation of LC3 than rapamycin.

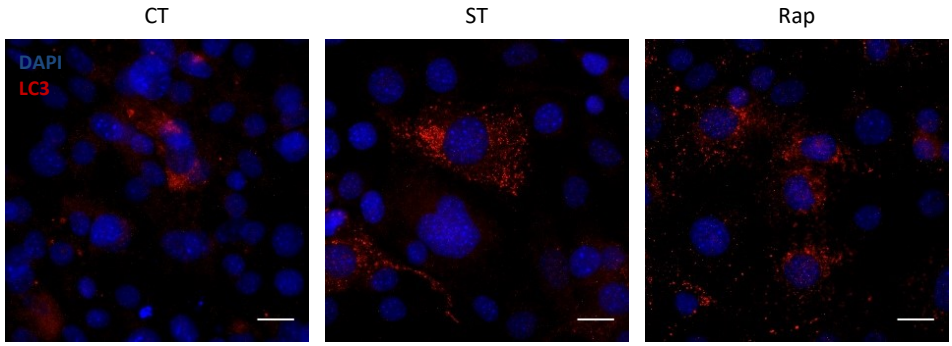

Figure 15. Starvation and rapamycin increase the formation of autophagic vesicles in MCEC-1.
The presence of LC3 was assessed by immunofluorescence in MCEC-1 subjected to 24 hours of starvation and rapamycin. Representative immunofluorescence images show an increase in LC3 presence and puncta positively stained for LC3. Nuclei were stained with DAPI. Scale bar: 50 µm. Data represents one independent experiment.

4.6. Simvastatin and rapamycin in the modulation of EC autophagy

4.6.1. Simvastatin induces the accumulation of Cx43 and autophagy protein markers MCEC-1

After proper characterization of the autophagy levels in MCEC-1, we proceeded to test the effect of rapamycin and simvastatin on this pathway. MCEC-1 were treated with 1 µM Simvastatin, 50 nM Rapamycin, added separately or concomitantly, for either 24 or 48 hours. Changes in the expression levels of proteins associated with autophagy were analysed by WB (Figure 16A).

After 24 hours of incubation with rapamycin, we observed an increase in AMPK protein levels (Figure 16B) whereas at 48 hours we detected a shift with an increase in Beclin-1 levels (Figure 16C). Longer periods of rapamycin, or concomitant simvastatin and rapamycin treatment, seem to decrease AMPK levels whereas Beclin-1 expression levels are increased. Based on these results, we can hypothesise that depending on the duration of mTOR inhibition, autophagy in MCEC-1 can be activated through different pathways, either AMPK or Beclin-1 dependent.

Results presented in Figure 16D and Figure 16E, respectively, shows that simvastatin incubation for 24 and 48 hours leads to an increase in p62 and LC3-II protein levels. This increase in autophagy-associated proteins can simultaneous indicate that simvastatin can induce autophagy flux or lysosome inhibition. On the other hand, LC3 levels seems to be increased in all treatment conditions after 24 hours, while after 48 hours, LC3 levels are only increased in the simvastatin alone condition, which may reflect an inhibition of autophagosome clearance. This may suggest a different autophagic pattern regarding these two autophagy-associated proteins and autophagy modulation within different time windows.

Taking into consideration Figure 16F, and in agreement with autophagy impairment induced by 24 and 48 hours of treatment with simvastatin, we also observe an increase in Cx43 protein levels under the same periods of simvastatin incubation. Taken together, this data showing that simvastatin is inducing the accumulation of proteins associated with autophagy activation (p62 and LC3-II) while also leading to an increase Cx43 protein levels, suggests that Cx43 constitutes is an autophagy substrate in this endothelial cell line.

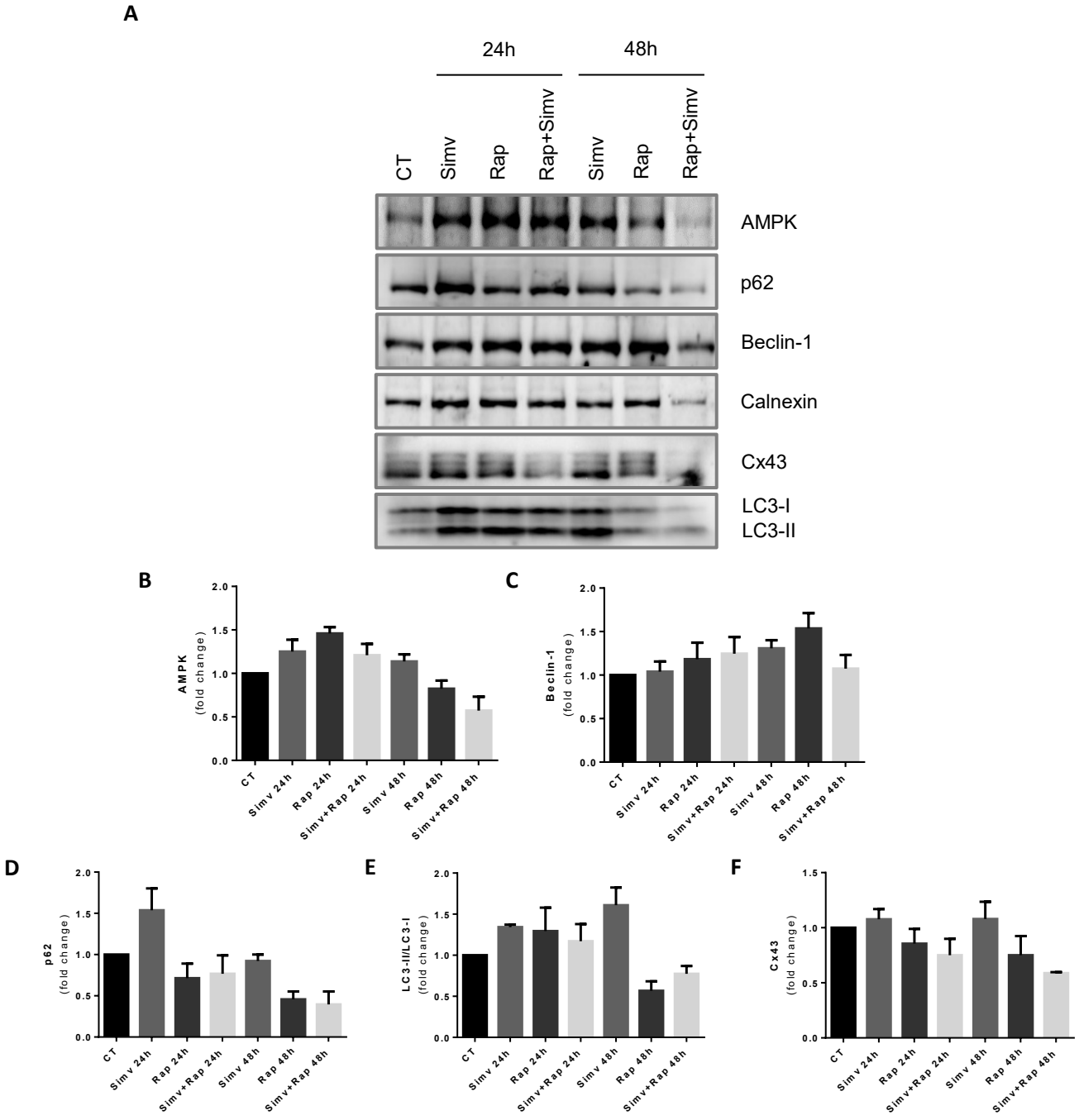

Figure 16. Simvastatin increases expression levels of p62, LC3-II and Connexin43.
(A) MCEC-1 were incubated with either 1 µM Simvastatin, 50 nM Rapamycin or both for either 24 or 48 hours and protein markers of autophagy were evaluated by WB analysis. Quantification of AMPK (B), Beclin-1 (C), p62 (D), LC3-II/LC3-I (E) and Cx43 (F) levels. Quantification of AMPK, Beclin-1, p62 and Cx43 was normalized using Calnexin as a loading control. Results represent mean ± S.D. of triplicate samples from three independent experiments.

4.6.1.1. Simvastatin induced accumulation of autophagy-associated proteins is increased by lysosomal inhibitors in MCEC-1

Results from simvastatin treatment suggest that simvastatin may be either promoting autophagy flux or inhibiting lysosomal degradation in MCEC-1. In order to tackle this question, we analysed the autophagic response of MCEC-1 in conditions where simvastatin treatment is combined with an autophagy inhibitor.

Cells were incubated for 24 hours either with 1 µM Simvastatin or 100 nM Bafilomycin A1 (Baf), or for 24 hours with 1 µM Simvastatin and 100 nM Bafilomycin A1 in the last 6 hours of treatment (Simv+Baf A). Levels of autophagic proteins were assessed by WB (Figure 17).

As expected, lysosomal inhibition by bafilomycin induces an accumulation of p62 and LC3-II, as seen in Figure 17B and Figure 17C, respectively. In agreement with the above data suggesting that Cx43 is a substrate of autophagy in MCEC-1, the accumulation of p62 and LC3-II in these conditions is accompanied by an accumulation of Cx43, as depicted in Figure 17D.

Simvastatin treatment increases both autophagy-associated proteins p62 and LC3-II. Furthermore, a deeper analysis of the results represented in Figure 17, reveals that simvastatin in not only increasing LC3-II levels but also LC3-I levels. Simultaneous incubation of simvastatin and lysosome inhibitor bafilomycin, leads to an increased accumulation of p62 and LC3-II compared with simvastatin treatment alone, but lower than the increase induced by lysosome inhibitors, which may suggest that simvastatin is partially inhibiting the lysosome activity and/or the fusion of the autophagosome with the lysosome in MCEC-1.

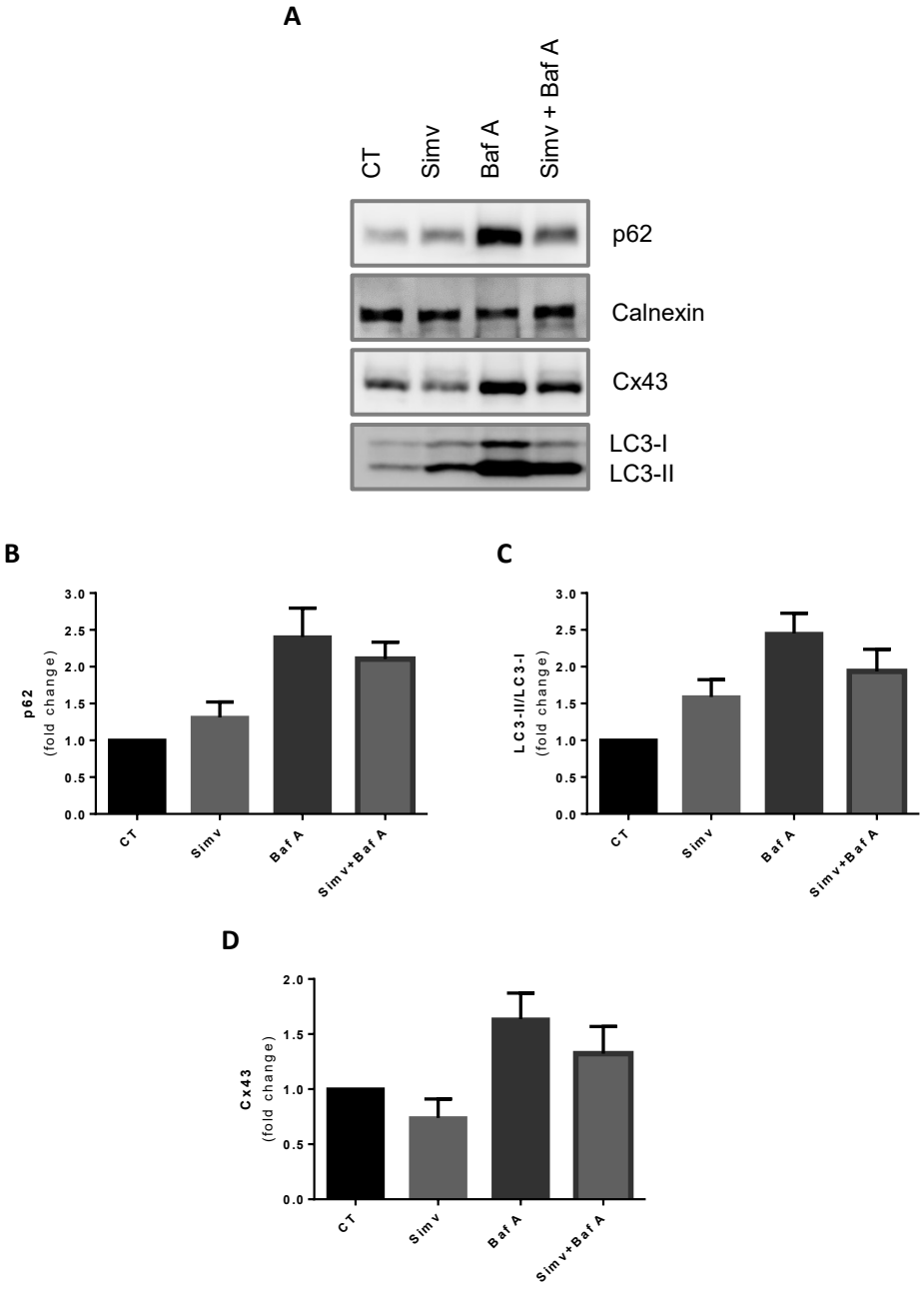

Figure 17. Effect of simvastatin and bafilomycin on autophagy in MCEC-1 cells.
MCEC-1 were incubated for 24 hours with 1 µM Simvastatin or 100 nM Bafilomycin A1 (Baf A), or with 1 µM Simvastatin for 24 hours and 100 nM Bafilomycin A1 in the last 6 hours. Differences in autophagy associated proteins were assessed by WB analysis. (A) Representative WB of protein levels of p62, LC3-I and LC3-II and Cx43. Quantification of p62 (B), LC3-II/LC3-1 (C) and Cx43 (D) protein levels. Quantification of p62 and Cx43 was normalized to Calnexin. Results represent mean ± S.D. of triplicate samples from three independent experiments.

4.6.2. Simvastatin induces an accumulation of LC3-II in PAEC

After assessing how simvastatin can modulate the autophagic pathway in the endothelial cell line, we decided to study if the autophagic response is similar in a primary cell culture. Thus, we replicated the experiments performed above in MCEC-1 in PAEC. Results in the form of WB analysis are depicted in Figure 18A.

Regarding AMPK, in Figure 18B we observe a gradual decrease in protein levels from 24 to 48 hours of treatment with simvastatin and with rapamycin, similar to the MCEC-1 response. However, changes in Beclin-1 protein levels do not seem to follow the same pattern observed in MCEC-1, with the levels of this protein decreasing after 48 hours of incubation with simvastatin, as represented in Figure 18C.

In agreement with the MCEC-1 response, in PAEC, the levels of p62 decrease in the first 24 hours of incubation with rapamycin and with the concomitant incubation of simvastatin and rapamycin. However, after these 24 hours of incubation, p62 levels recover, as demonstrated in Figure 18D, whereas in MCEC-1 p62 protein levels further decreased after 48 hours of incubation, which may indicate a different response pattern in PAEC.

Similar to MCEC-1, incubation with simvastatin for 48 hours resulted in the accumulation of LC3-II (Figure 18E) while the other experimental conditions tested did not seem to affect LC3-II protein levels relative to controls. Cx43 on the other hand, accumulated during shorter periods of treatments as represented in Figure 18F.

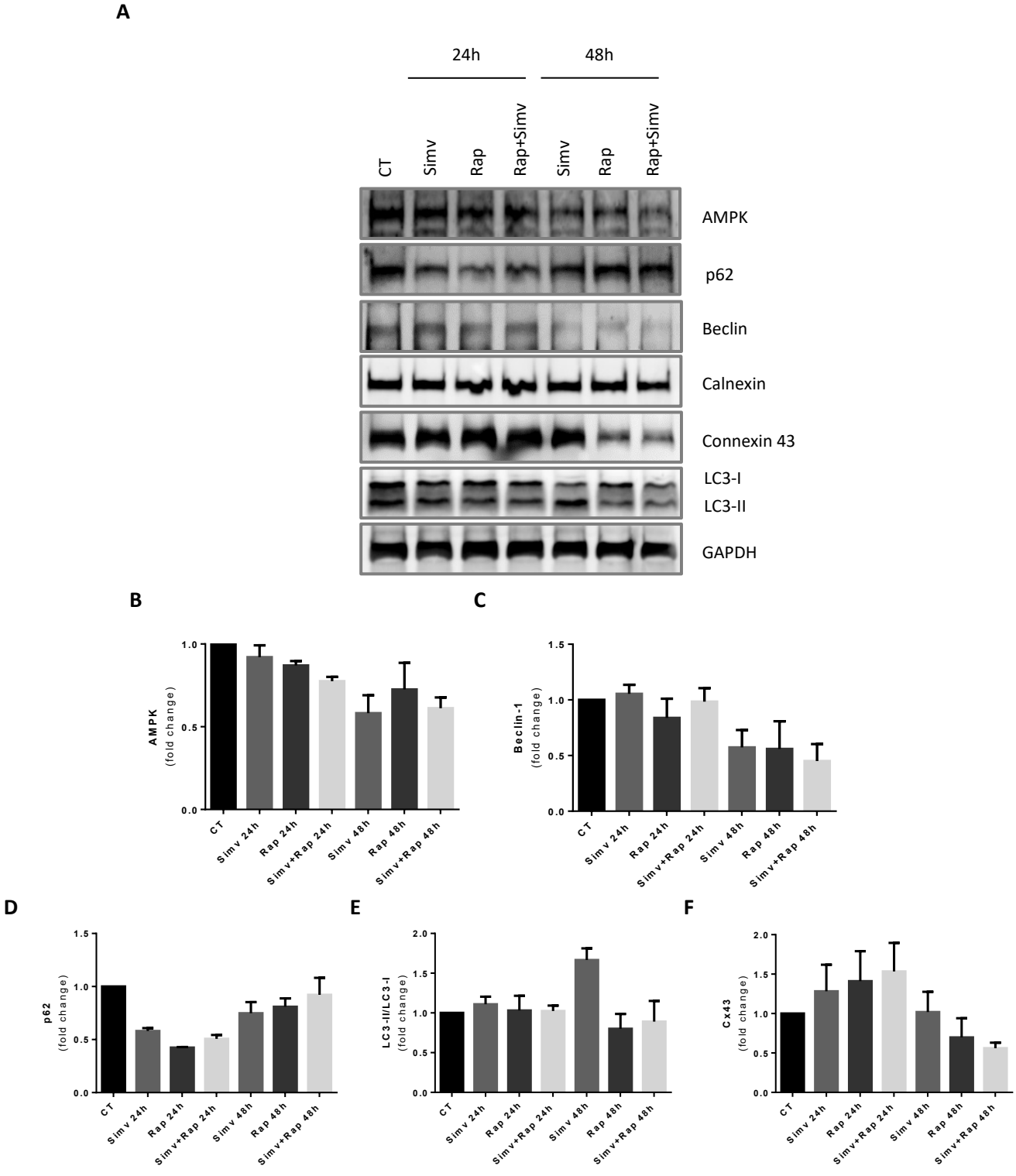

Figure 18. **Simvastatin induces the accumulation of LC3-II in PAEC.**
PAEC were incubated with 1 µM Simvastatin, 50 nM Rapamycin or both, for either 24 or 48 hours and protein markers of autophagy were evaluated by WB analysis. (A) Representative WB of protein levels of AMPK, Beclin, p62, LC3-I and LC3-II and Cx43. Quantification of AMPK (B), Beclin-1 (C), p62 (D), LC3-II/LC3-I (E) and Cx43 (F) protein levels. Quantification of AMPK, Beclin-1, p62 and Cx43 levels was normalized to GAPDH. Results represent mean ± S.D. of triplicate samples from three independent experiments.

4.6.2.1. Simvastatin induced accumulation of autophagy-associated proteins is increased by lysosomal inhibitors in PAEC.

Similar to the experiments described earlier for MCEC-1, we also investigated the impact of simvastatin upon autophagy activity in PAEC. Cells were incubated for 24 hours either with 1 µM Simvastatin or 100 nM Bafilomycin A1 (Baf A), or for 24 hours with 1 µM Simvastatin and 100 nM Bafilomycin A1 in the last 6 hours of treatment (Simv+Baf A). Levels of autophagic proteins were assessed by WB (Figure 19A).

As expected, lysosomal inhibition by bafilomycin leads to an accumulation of p62 and LC3-II, as represented in Figure 19B and Figure 19C, respectively. Cx43 protein levels (Figure 19D), also increase under bafilomycin addition, indicating that Cx43 is also a substrate of autophagy in PAEC.

Regarding the effect of simvastatin in autophagy modulation, similar to MCEC-1, data shows that the conjugation of simvastatin with a lysosome inhibitor leads to the accumulation of p62 compared with simvastatin treatment alone. However, the effect of simvastatin treatment alone in MCEC-1 differs from PAEC, since in MCEC-1 simvastatin incubation leads to an accumulation of p62 whereas in PAEC it leads do a decrease in the protein levels of this autophagy adaptor. In the case of LC3, simvastatin treatment induces a slight increase in LC3 levels, which are further enhanced when PAEC are incubated with simvastatin and a lysosomal inhibitor (Simv+Baf A). Contrary to what happens in MCEC-1, treatment of PAEC with Simv+Baf A leads to an accumulation of LC3-II to levels that are similar to those of cells exposed to Baf A alone. Nevertheless, the slightly increased LC3-II levels after simvastatin incubation, suggest that also in PAEC, simvastatin may be partially inhibiting the lysosome activity and/or the fusion of the autophagosome with the lysosome but in a more attenuated manner.

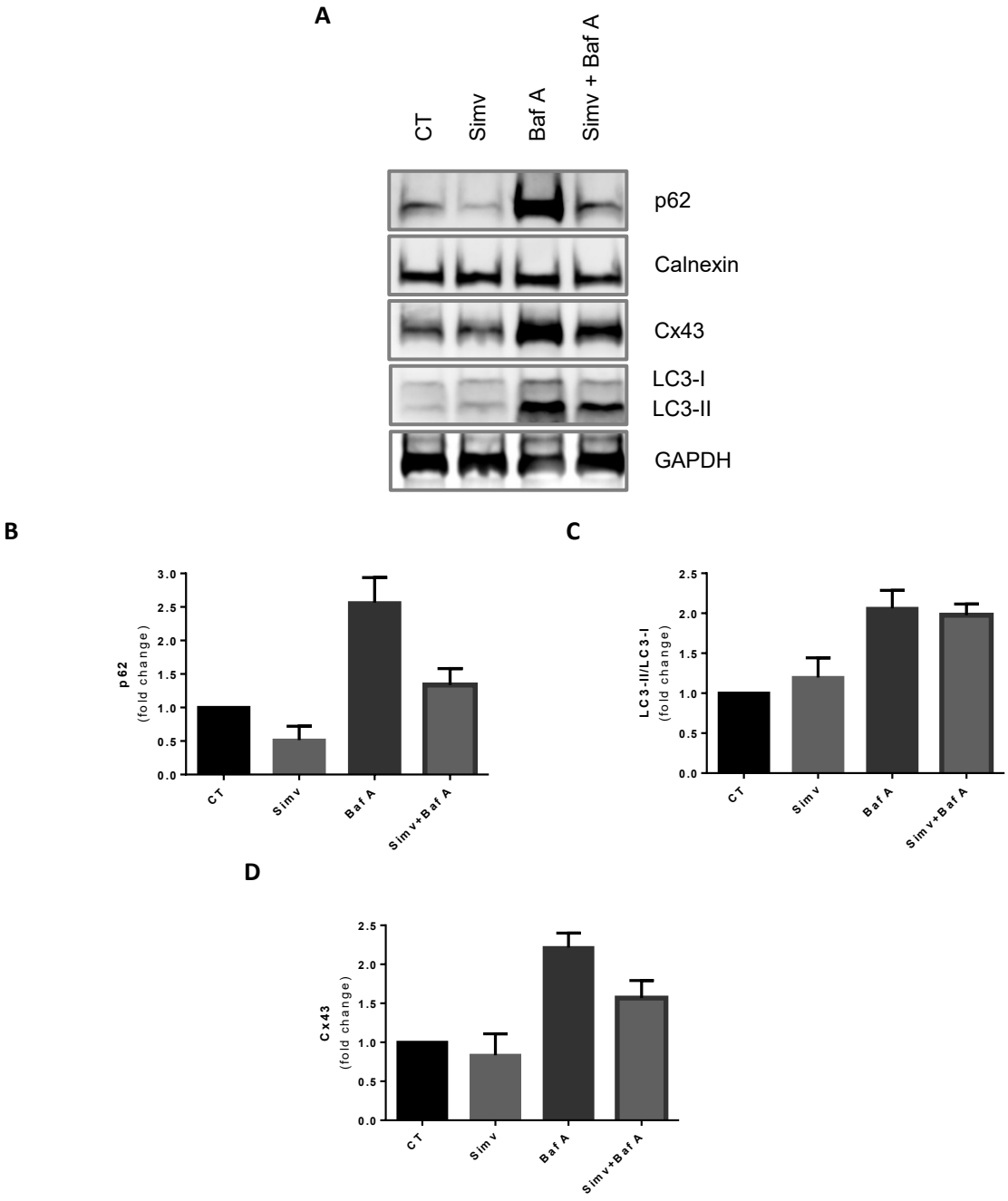

Figure 19. Effect of simvastatin and bafilomycin A on autophagy in PAEC cells.
PAEC were incubated for 24 hours with 1 µM Simvastatin or 100 nM Bafilomycin A1 (Baf A), or with 1 µM Simvastatin for 24 hours and 100 nM Bafilomycin A1 in the last 6 hours. Differences in autophagy associated proteins were assessed by WB analysis. (A) Representative WB of protein levels of p62, LC3-I and LC3-II and Cx43. Quantification of p62 (B), LC3-II/LC3-I (C) and Cx43 (D) protein levels. Quantification of p62 and Cx43 levels was normalized to Calnexin. Results represent mean ± S.D. of triplicate samples from three independent experiments.

4.7. Modulation of autophagy in SMC by simvastatin and rapamycin

4.7.1. SMC isolated from porcine aortae positively stains for α-smooth muscle actin.

After characterizing the effect of simvastatin and rapamycin upon EC autophagy, we proceeded to test the response of SMC to these compounds. Smooth muscle cells from the media layer of fresh porcine aortae were isolated, grown on coverslips, and then immunostained for α-smooth muscle actin (α-SMA) to ensure the presence of SMC in the cell culture.

Data presented in Figure 20 demonstrates that the cells obtained from pig aortae positively stains for α-SMA, confirming the presence of SMC. A more deep analysis of the immunofluorescence images reveals that not all cells positively stains for α-SMA, indicating some impurity in the cell culture. Additionally, cells present in the isolated culture positively stain for Cx43, a protein that is present in SMC.

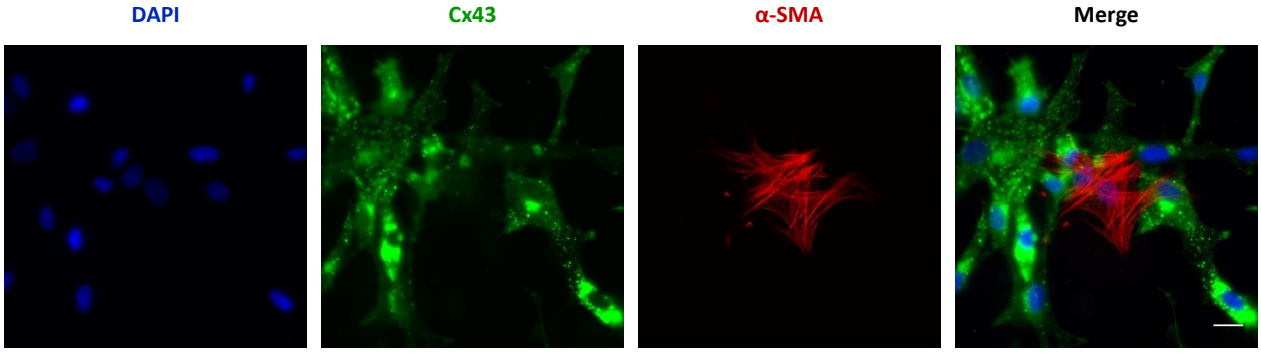

Figure 20. Smooth muscle cells obtained from porcine aortae positively stains for α-SMA.
Representative immunofluorescence images of cells obtained from pigs aortae were seeded and stained for Cx43 and α-SMA. Images were analysed using ImageJ. Scale bar 50 μm.

4.7.2. Rapamycin and simvastatin modulate autophagy-associated proteins in SMC

After confirming that our cell cultures contain SMC, we proceeded to study the autophagic response to simvastatin and rapamycin in the same conditions described earlier for MCEC-1 and PAEC. SMC were incubated with either 1 µM Simvastatin, 50 nM Rapamycin or both for 24 and 48 hours. Results were assessed using WB analysis as shown in Figure 21A.

Analysing Figure 21B, AMPK protein levels seems to increase after 24 hours of rapamycin incubation and to decrease after 48 hours of incubation with simvastatin alone or together with rapamycin. Both results are in accordance with what was observed for MCEC-1 and PAEC.

Surprisingly, SMC treated with rapamycin alone or together with simvastatin, display an initial increase in p62 levels at 24 hours of treatment, which then decreases below control levels after 48 hours (Figure 21C). This pattern in SMC p62 levels is contrary to what was found in EC as described above. LC3-II (Figure 21D) and Cx43 (Figure 21E) display the same pattern of variation when treated with rapamycin alone, which may suggest that, similar to EC, in SMC Cx43 also constitutes an autophagy substrate. Furthermore, and contrary to what was observed in MCEC-1, LC3-II accumulates when SMC are incubated for 48 hours with rapamycin alone or together with simvastatin.

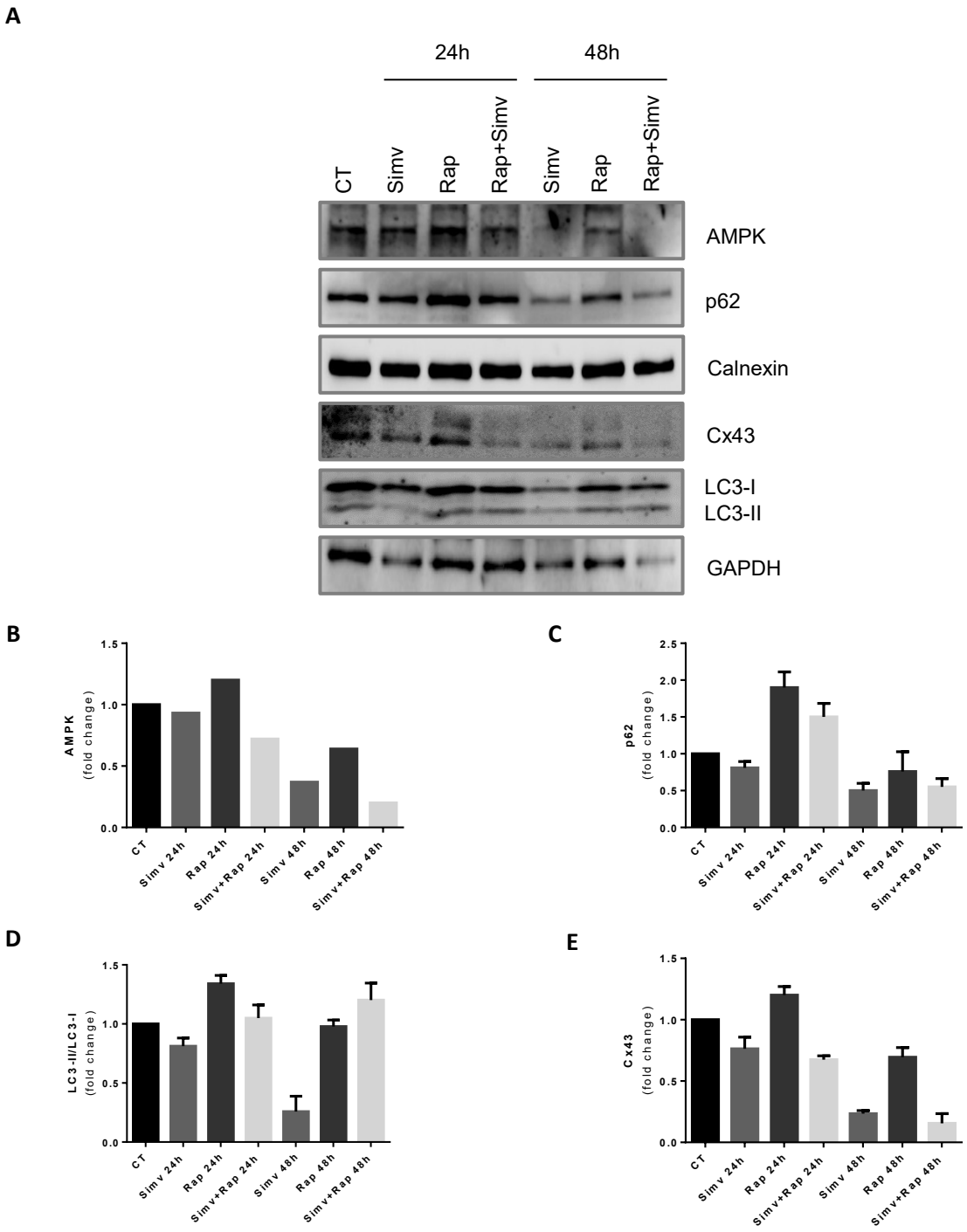

Figure 21. Modulation of autophagic proteins by simvastatin and rapamycin in SMC.
SMC were incubated with 1 µM Simvastatin, 50 nM Rapamycin or both, for either 24 or 48 hours and protein markers of autophagy were evaluated by WB analysis. (A) Representative WB of protein levels of AMPK, p62, LC3-I and LC3-II and Cx43. Quantification of AMPK (B), p62 (C), LC3-II/LC3-I (D) and Cx43 (E) protein levels. Quantification of AMPK, p62 and Cx43 was normalized to GAPDH. Results represent mean ± S.D. of triplicate samples from two independent experiments, except for AMPK, which results from one independent experiment.

4.7.2.1. Simvastatin induced accumulation of autophagy-associated proteins is increased by lysosomal inhibitors in SMC

The ability of statins to inhibit SMC migration and proliferation through autophagy activation has been described in the literature[54,67,71]. Therefore, we wanted to clarify whether simvastatin was being able to induce autophagy in our SMC culture obtained from porcine aortae. To answer this question, we subjected these cells to the same experimental conditions as MCEC-1 and PAEC. Cells were incubated for 24 hours either with 1 µM Simvastatin or 100 nM Bafilomycin A1 (Baf), or for 24 hours with 1 µM Simvastatin and 100 nM Bafilomycin A1 in the last 6 hours of treatment (Simv+Baf A). Levels of autophagic proteins were assessed by WB (Figure 22A).

As expected, bafilomycin treatment increases p62 and LC3-II protein levels (Figure 22B and 22C). This increase in accompanied by an accumulation of Cx43 (Figure 22D), indicating that in SMC, Cx43 is also a substrate of autophagy.

Regarding simvastatin treatment, it induces an accumulation of p62 and LC3-II protein levels, and this accumulation is even greater when the lysosome inhibitor is added. However, this accumulation is inferior to the levels observed when cells are treated with Baf A alone. Furthermore, Cx43 levels decrease when cells are treated with simvastatin alone.

Taken together, this data seems to suggest that simvastatin may be inducing lysosomal activity inhibition thus accumulating proteins markedly associated with autophagy and/or inhibiting autophagosome-lysosome fusion.

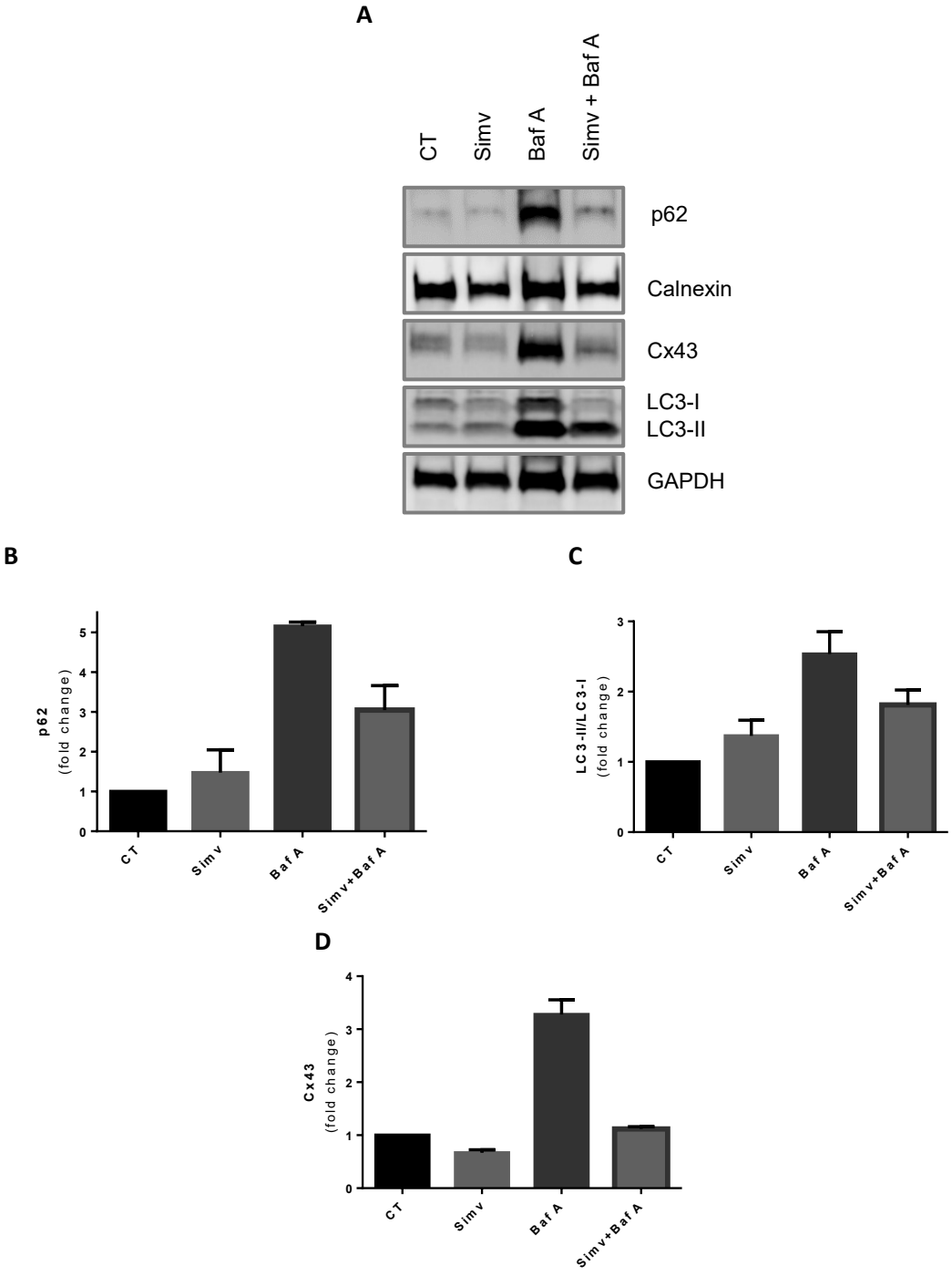

Figure 22. Effect of simvastatin and bafilomycin A on autophagy in SMC cells.
PAEC were incubated for 24 hours with 1 µM Simvastatin or 100 nM Bafilomycin A1 (Baf), or with 1 µM Simvastatin for 24 hours and 100 nM Bafilomycin A1 in the last 6 hours. Differences in autophagy associated proteins were assessed by WB analysis. (A) Representative WB of protein levels of p62, Cx43, LC3-I and LC3-II. Quantification of p62 (B), LC3-II/LC3-I (C) and Cx43 (D) protein levels. Quantification of p62 and Cx43 was normalized to either Calnexin or GAPDH. Results represent mean ± S.D. of triplicate samples from two independent experiments.

5. Discussion

The heart is a muscular organ constituted by a variety of cell types, including cardiomyocytes, fibroblasts, endothelial cells, smooth muscle cells, immune cells, pacemaker cells and Purkinje cells[1]. The main function of the heart is to pump blood through all the blood vessels of the circulatory system, thus delivering oxygen and nutrients to all tissues and organs of the organism. The contraction and relaxation capacity of the heart relies on a cardiac muscle, the myocardium, being the heartbeat rhythm mainly dictated by cells with autonomous contractile capacity localized in specific regions of the heart called AV- and SA nodes, called for this reason the pacemaker cells. To contract in a synchronised and coordinated manner as a whole, the electrical impulses generated on these nodes have to be rapidly and efficiently propagated to the rest of myocardium, allowing the heart to work as a functional syncytium. For that, the heart relies on a complex network of low resistance channels that ensure intercellular communication between cardiomyocytes, called gap junction channels.

Defects in GJ-mediated intercellular communication have been implicated in the development of vascular pathologies, such as atherosclerosis and restenosis[74,75]. GJ are formed by connexins and particularly Cx43, which is the most abundantly expressed in the heart[2], has been suggested to be involved in restenosis and neointima hyperplasia development[76,77]. In fact, it was reported that Cx43 is upregulated in vessels subjected to balloon angioplasty and after Cx43 knockdown, the balloon-induced restenosis and neointima hyperplasia was prevented[76].

The most common treatment of CAD is balloon angioplasty followed by stent implantation within the narrowed artery. However, the balloon inflation immediately leads to endothelium denudation that subsequently triggers a cascade of pathological events. Since one of the main biological functions of EC is to supress SMC proliferation, the decrease in EC population found within the stented area allows SMC to proliferate, ultimately resulting in neointima formation. Sirolimus, an analogue of rapamycin and a potent cytostatic agent, has been eluted in stents (SES) and has shown to be efficient inhibiting SMC migration and proliferation trough cell cycle arrest. However, it was described that sirolimus impairs EC migration and proliferation from intact neighbouring artery segments, which has been associated with the inhibition of re-endotheliazation and the restoration of an intact endothelium[42,78–80].

HMG-CoA reductase inhibitors, commonly known as statins, have been described to limit neointima formation[81], however the underlying mechanisms remain largely obscure. Additionally, statins have proved able to ameliorate endothelial function[67,68] and to enhance EC migration and proliferation primely impaired by sirolimus administration[71].

In this study we aimed to elucidate the mechanisms whereby simvastatin could revert the endothelial impairment induced by the rapamycin analogue sirolimus present in DES. To address this question, we used a microvascular neonatal mouse cardiac endothelial cell line MCEC-1 and primary cultures of pulmonary arterial endothelial cells, PAEC, incubated with rapamycin and/ or simvastatin.

Previous studies showed that in cardiac microvascular endothelial cells pre-treated with 1 nM Rapamycin, a concentration of 1 µM Simvastatin has significantly enhanced migration capacity[82]. In the migration assays performed in our work, the incubation of 50 nM Rapamycin significantly induced MCEC-1 to migrate more than 1 µM Simvastatin (Figure 8). Moreover, we show that the migration of MCEC-1 is enhanced in cells co-treated with simvastatin and rapamycin when compared to cells incubated with simvastatin. Since in our experimental model we aimed to mimic *in vivo* conditions, the differences obtained in our migration outcomes compared with the pattern found in the literature, may be explained by the higher dose of rapamycin used in our treatments. Nevertheless, there is a tendency for the combined treatment of rapamycin and simvastatin to attenuate simvastatin-induced migration delay, resulting in a half term between rapamycin and simvastatin-induced migration. Data obtained with PAEC demonstrates a similar tendency for simvastatin at low concentration to impair migration (Figure 9). However, 5 µM Simvastatin produces a better outcome than 1 µM Simvastatin and the co-treatment of rapamycin and simvastatin do not induce much greater migration than simvastatin itself. Concordantly with the described dose-dependent effect of statins[83], the effect of simvastatin in MCEC-1 migration, seems to follow the same dose-dependent pattern, since higher concentrations, namely 5 and 10 µM, delays migration. However, the same does not seem to apply in PAEC. Increased concentrations of simvastatin, particularly 5 µM, appears to exert more beneficial effects in migration capacity than a lower one, which may suggest a different response in MCEC-1 and in PAEC. A more deeply analysis of the data, reveals that MCEC-1 take longer to efficiently migrate towards wound closure (24 hours) than PAEC, that need only 8 hours to completely cover the scratch. Considering these data, we

can hypothesise that MCEC-1 and PAEC differ in migration patterns and that the response to simvastatin does not follow the same dose-dependent pattern, suggesting that a combination of rapamycin with a higher dose of simvastatin could enhance PAEC migration.

Statins, even under the presence of sirolimus, were demonstrated to improve EC proliferation[71,82]. Results from our study show that the conjugated treatment of rapamycin and sirolimus fails to overcome the proliferation impairment induced by the statin in MCEC-1 (Figure 10), and slightly overcomes in PAEC (Figure 11). Similarly to migration, both in MCEC-1 and PAEC rapamycin is responsible for the best outcomes in terms of proliferation rates. On the other hand, for all the concentrations tested simvastatin leads to a decrease of cell proliferation, that is not reverted by the presence of simvastatin. Interestingly, in MCEC-1, the increase in simvastatin concentrations represents a decreased proliferative profile, whereas in PAEC increased concentrations of simvastatin increases proliferation capacity. These results are concordant with the pattern found in the migration assay, in which a lower concentration of simvastatin produces a better effect in MCEC-1 migration capacity than increased ones, whereas in PAEC, the higher concentrations of this statin are responsible for better outcomes. With this in mind, it is conceivable that a combined treatment of rapamycin with a higher concentration of simvastatin than the one tested in our work, could exert increased beneficial effects in PAEC proliferation rates.

Angiogenesis, the capacity of pre-existing blood vessels to sprout new capillaries, largely depends on tissue integrity[66]. Therefore, the disruption of vascular integrity has been widely implicated in defective angiogenesis after balloon angioplasty. Statins effect in angiogenesis is dose-dependent[83–86], and in low concentrations, have shown beneficial effects in EC, particularly enhancing vascular-like structures formation *in vitro*[85]. In agreement, our results show that simvastatin incubation enhances tube formation in MCEC-1 either in presence or absence of a BMS, resulting in an increase of the number of nodes, meshes and in the length of master segments (Figure 12). Sirolimus has been described to impair angiogenic potential of EC, a major drawback after SES implantation. Our experimental model confirms the deleterious effect of this drug, decreasing the majority of the parameters evaluated. Indeed, our results show that both rapamycin and SES induce a decrease of number of nodes and meshes formed by MCEC. However, rapamycin-induced harmful effect, either in form of rapamycin incubation or in the form of a piece of SES, is reverted with the addition of a low dose of simvastatin, which suggests a

cooperative effect between rapamycin and simvastatin in MCEC-1. Statins have been reported to possess both pro- and anti-angiogenic properties depending on the concentration, and low doses of statins, as those found *in vivo,* seems to induce a pro-angiogenic phenotype[86], which is concordant with the results we obtained in MCEC-1. However, this simvastatin-induced enhancement of tube formation by low concentrations, does not seem to exert the same effect in PAEC, cumulatively suggesting a different dose-dependent response (Figure 13). Although with different amplitude, the impact of simvastatin and rapamycin in tubulation pattern is similar in both cell types, with simvastatin being either pro-angiogenic (MCEC-1) or presenting a modest effect (PAEC), whereas in the presence of rapamycin, either alone or with simvastatin, the tubulation capacity of both cells is lower in comparison with cells incubated with simvastatin. In PAEC, the addition of simvastatin to the rapamycin treatment, either in the form of the drug incubated in the matrigel or in the form of a piece of SES entrapped within the matrigel, fails to overcome rapamycin-induced tube formation impairment. It is plausible that differences in cell response to simvastatin and rapamycin rely on differences on the cell types, since MCEC-1 are microvascular cardiac endothelial cell whereas PAEC are primary cultures of pulmonary arterial origin. Moreover, it is possible to hypothesize that higher concentrations of simvastatin, combined with sirolimus, may be able to modulate angiogenesis *in vivo* thus serving as a therapeutic approach.

Being a rapamycin analogue, sirolimus affects mTOR, with a consequent impact on autophagy. Therefore, we hypothesised that the detrimental effects of sirolimus on EC after stent deployment could be due to an impact on autophagy. To address this question, we first characterised the autophagy activity in MCEC-1, which had not been described before (Figure 14). Our results reveal that this endothelial cell line possesses an active autophagy pathway. For instance, when MCEC-1 are subjected to starvation, which is a common way to trigger autophagy since it inhibits mTOR activity[53], and subjected to a more severe form of amino acids deprivation (HBSS), we observed a decrease of phosphorylated mTOR levels, p-mTOR, which indicates a decreased activity of mTOR and subsequently autophagy activation. As mentioned above, rapamycin is a well described mTOR inhibitor and has proved to activate autophagy both *in vitro* and *in vivo*[87]. In the endothelial cell line tested in this work, rapamycin exerts the same inhibitory effect in mTOR, confirmed by the decrease in p-mTOR expression levels upon rapamycin incubation. Under the same

experimental conditions, we observe a decrease in autophagy adaptor p62 protein levels and in the ratio of LC3-II/LC3-I, concordantly with the activation of autophagy and consequent lysosomal degradation, diminishing p62 and LC3-II levels. Starvation seems to be increasing LC3-I to LC3-II conversion as demonstrated by the slight accumulation of LC3-II. As described[88], the lysosomal turnover of LC3-II can be used as a reflection of starvation-induced autophagic activity and thus, this may suggest that starvation is inducing an increased LC3-I conjugation to phosphatidylethanolamine, which indicates increased autophagosome formation. This was confirmed by immunofluorescence, where MCEC-1 subjected to starvation led to puncta formation that positively stains for LC3, suggesting an enhancement of autophagic vesicles formation (Figure 15). Moreover, as a proof of concept, it is described in the literature that under basal conditions LC3 is found evenly distributed in both the nucleus and the cytoplasm, and that under nutrient-deprived conditions, LC3 suffers a redistribution from the nucleus to the cytoplasm[89]. Similarly, in the control condition we observe LC3 uniformly distributed, while in cells subjected to starvation is notorious an increased accumulation of LC3 in the cytoplasm. Also rapamycin demonstrates to be inducing autophagy, observed by the increasing LC3 puncta in this experimental condition. MCEC-1 positively responds to lysosomal inhibitors by accumulating the autophagy adaptor p62 and the autophagosome marker LC3-II. To confirm the activation of autophagy by starvation, HBSS or rapamycin we evaluated the levels of Cx43, a well-established substrate of autophagy[90,91]. As expected, we observed a decrease of Cx43 in MCEC-1 cells subjected to both types of starvation or treated with rapamycin, that was reverted by lysosomal inhibition.

After autophagy been characterised, we proceeded testing simvastatin and simvastatin and rapamycin conjugated treatment in autophagic response (Figure 16). Several studies have shown statins capacity to activate autophagy[92–95]. In coronary arterial monocytes, simvastatin enhanced autophagy through conversion of LC3-I in LC3-II and by increased expression of Beclin-1, and this autophagy activation exerted a protective effect in atherosclerosis[95]. In HL-1 cardiomyocytes, simvastatin treatment for 24 hours resulted in mTOR signalling suppression and in a consequent upregulated autophagy[92]. Other studies describe statins capacity to indirectly downregulate mTOR phosphorylation through upregulation of AMPK phosphorylation[96].

The results obtained in this study show that simvastatin incubation for 24 hours in MCEC-1 leads to an accumulation of LC3-II and p62, which may suggest either an enhanced autophagosome formation, responsible for the increased conversion of LC3-I in LC3-II, or an inhibitory effect of simvastatin in lysosomal degradation, thus accumulating p62. After 48 hours of treatment, p62 seems to be restored to basal levels while LC3-II/LC3-I ratio levels remain increased, even accumulating a higher amount than in 24 hours of treatment. Since p62 expression levels at 48 hours are similarly to the control condition, it seems that at that time simvastatin is not exerting any effect, at least, regarding lysosome degradation impairment, because if so, p62 would continue to accumulate. With these data we can hypothesise that simvastatin may be promoting autophagosome formation through increased conversion of LC3-I into LC3-II, suggesting an activation of autophagy, however the fusion of these autophagosomes with the lysosome is impaired. It has been shown that simvastatin induces p62 synthesis through the activation of ERK/JNK pathway. Therefore, it is plausible that the effect of simvastatin in p62 levels is mediated by an autophagy-independent process.

In PAEC we found the same pattern in LC3-II expression levels, in which 24 hours of incubation leads to an increase in LC3-II levels and for a longer period, this accumulation is even greater (Figure 18).

It has been described that autophagy activation can be mediated by different pathways, involving diverse players, namely AMPK and Beclin-1[44,51]. Interestingly, our results show that incubation with simvastatin for 24 hours resulted in an increase of AMPK, that recover to basal levels after 48 hours, which coincides with an increase of Beclin-1. These data suggest that the mechanisms underlying autophagy activation are different along the period of incubation with simvastatin.

To further characterize the effect of simvastatin in autophagy, we compared the LC3 levels either in the presence or absence of lysosome inhibitors (Figure 17). As expected, bafilomycin treatment is responsible for a massive accumulation of p62 and LC3-II. However, the addition of this lysosome inhibitor to simvastatin results in a mid-term of p62 and LC3-II accumulation levels between the simvastatin and bafilomycin treatments alone. Nevertheless, simvastatin and bafilomycin were independently incubated for 24 hours. In the case of the co-treatment of simvastatin and the lysosome inhibitor, simvastatin was also incubated for 24 hours whereas bafilomycin was added only in the last 6 hours of the

experiment, not exerting the same level of lysosome inhibition as if bafilomycin was incubated for 24 hours. Thus, the mid-term accumulation of p62 and LC3-II under the simvastatin and lysosome inhibitor treatment, reflects the inhibition of the lysosome only in the last hours of treatment. While the increase in p62 and LC3-II protein levels induced by simvastatin may indicate that autophagy is being activated, thus leading to the accumulation of these proteins, it is interesting to note that adding the autophagy inhibitor to simvastatin treated cells does not lead to an additive effect. These results suggest that autophagy flux is not being induced by simvastatin, but rather an impairment of autophagosome fusion with the lysosome is occurring. Moreover, these results open up the possibility that simvastatin treatment, in addition to partially affecting last steps of autophagy, may also be inducing the degradation of p62 and LC3-II through a pathway that is not sensitive to bafilomycin treatment in MCEC-1. Contrary to what happens in MCEC-1, treatment of PAEC with simvastatin and with a lysosome inhibitor leads to an accumulation of LC3-II to levels that are similar to those of cells exposed to bafilomycin alone, suggesting that in these cells the effect of simvastatin is at the level of lysosome function (Figure 19). In the case of p62, and similar to MCEC-1, it is possible that simvastatin treatment induces the degradation of p62 through autophagy independent pathways, namely by the UPS.

Interestingly, the treatment of SMC with simvastatin decreased the levels of both p62 and LC3-II, suggesting that, contrary to what was observed in EC, simvastatin is promoting or accelerating the fusion of autophagosomes with the lysosome (Figure 21). However, simvastatin during the same period of incubation represented in Figure 22, denotes an increase in the levels of these marker autophagy proteins. This discrepancy in p62 and LC3-II levels may be justified by the different passages of SMC used in these two experiments. As expected, also in SMC bafilomycin treatment increases p62 and LC3-II protein levels (Figure 22). Similarly to MCEC-1 and PAEC, SMC concomitantly treated with simvastatin and bafilomycin, led to an accumulation of p62 and LC3-II that is higher than in cells treated with simvastatin alone, but lower than those treated with bafilomycin. Furthermore, Cx43 levels decrease when cells are treated with simvastatin alone. Taken together, this data strengthens our hypothesis that simvastatin can be affecting lysosomal activity and/or autophagosome-lysosome fusion. However, it is important to note that when SMC are treated with simvastatin alone for 48 hours (Figure 21), there is a remarkable decrease in p62, and especially in LC3-II levels, suggesting a consumption of LC3-II likely

due to an upregulation of that autophagy. Thus, while it is possible that the increase in p62 and LC3-II levels observed after 24 hours of simvastatin treatment is due to autophagy inhibition, alternatively, this may reflect a temporary upregulation of p62 and LC3-II in order to respond to an increase in autophagic activity. It is also plausible that a decrease in p62 and LC3-II levels is associated with inhibition of transcription or translation of these proteins. Importantly, this effect of simvastatin appears to be unique to SMC, as MCEC-1 and PAEC were either unresponsive to 48 hours of simvastatin treatment, or displayed increased levels of p62 and LC3-II. This is not surprisingly since it has been established that the conversion of LC3-I to LC3-II is not only dependent on the stimuli used to activate autophagy, but is also cell-type specific.

Several studies have demonstrated that statins decrease the content of cholesterol in the plasma membrane of some cell types and, moreover, the mTOR has been suggested to be involved in sensing changes in cholesterol concentrations in endothelial cell[97,98]. The presence of cholesterol in the plasma membrane is responsible for conferring adequate fluidity and selective permeability to cellular membranes and constitutes an essential component in lipid rafts[99]. The cell possesses two sources of cholesterol, either acquiring LDL from the extracellular space through receptor-mediated endocytosis[100] or by its synthesis in the endoplasmic reticulum[101]. Regardless the source of cholesterol chosen by the cell, a proper cholesterol homeostasis at the plasma membrane is essential to control its structure and function. Assuming that the statin focused in this work, simvastatin, is able to exert the same effect in EC, we can hypothesize that an altered amount of this lipid may change the fluidity of the plasma membrane, becoming less selective to what is allowed to enter the cell. Consequently, some macromolecules that in normal conditions would not be internalized, may diffuse through the plasma membrane, activating autophagy through mTOR inhibition, inducing autophagosome formation and an increase in conversion of LC3-I to LC3-II. In the literature, is described that blocking cholesterol exit from endosomal/lysosomal compartments to the plasma membrane, may lead to inhibition of mTOR[98]. Additionally, there are evidences that the mTOR activity in EC requires proper cholesterol trafficking and the blockade of cholesterol trafficking through lysosome has been described to inhibit mTOR activity[98].

Besides the blockage of mevalonate synthesis and its effect in inhibiting cholesterol synthesis, statins inhibition of mevalonate pathway also provides isoprenoids for

prenylation of different proteins, including proteins involved in autophagy, such as Rab7, that is required for the maturation of late autophagosomes and its fusion with lysosomes. It was previously shown that N6-isopentenyladenosine (iPA), which constitutes an end product of the mevalonate pathway and that is also responsible for protein prenylation, prevents the autophagosome–lysosome fusion through unprenylated Rab7[102]. Thus, this product of mevalonate pathway impairs the autophagic flux by inhibiting autophagosome-lysosome fusion. Since a proper autophagic flux relies in an equilibrium between autophagosome formation and its clearance by the lysosomes, it is conceivable that simvastatin, due to inhibition of the mevalonate/isoprenoid pathway inhibition, may also impair the late autophagosome–lysosome fusion step of autophagy, constituting a late-stage inhibitor of autophagy in EC.

6. Concluding remarks

With this work we demonstrate that, in the mouse cardiac endothelial cell line MCEC-1, the treatment with a low concentration of simvastatin impairs migration capacity and this impairment is reverted when simvastatin is concomitantly incubated with rapamycin. In human pulmonary arterial endothelial cells, PAEC, simvastatin also delays migration but the co-treatment with simvastatin and rapamycin does not overcome the simvastatin-induced migration impairment. Nevertheless, there is a tendency for higher doses of simvastatin to increase migration, opening up the possibility that rapamycin combined with higher concentrations of simvastatin could enhance EC migration capacity.

Regarding proliferation, and similarly to migration, simvastatin at low doses decreases MCEC-1 and PAEC proliferation rates and the combined treatment of rapamycin and simvastatin is not efficiently reverting the simvastatin-induced proliferation impairment. However, once again PAEC demonstrates a propensity to respond better under higher doses of simvastatin than to lower ones. Thus, we can hypothesise that a co-treatment of rapamycin with an increased concentration of simvastatin than the one tested, could improve PAEC proliferation.

In this study we show that simvastatin is able to increase tubulation in MCEC-1. Moreover, when simvastatin is added to cells treated in the presence either of rapamycin or a piece of SES, this statin efficiently reverts the deleterious effect induced by rapamycin or the SES, respectively. In PAEC this effect is not observed, though in this experiment, increased concentrations of simvastatin were not tested. In further studies, it should be assessed the hypothesis that the combined treatment of rapamycin with a higher dose of simvastatin may exert a cooperative effect in migration, proliferation and tube formation of EC.

The characterisation of the autophagy pathway in the endothelial cell line used in this work, constitutes an important novelty that enables further autophagy-related studies. Namely, MCEC-1 positively responds to different types of autophagy-activation inducers, either starvation or rapamycin, suggesting an autophagy activation through mTOR inhibition. Moreover, protein levels of Cx43, a well-established autophagy substrate, decrease under treatment with autophagy-activation inducers whereas in the presence of lysosome inhibitors, it accumulates.

Overall, this study demonstrates that the effect of simvastatin and rapamycin regarding cell migration, proliferation and angiogenesis capacity is endothelial cell-type specific. Moreover, our results demonstrate that these compounds exert different impacts an autophagy of ECs and SMC.

The results presented in this work not only present novelty but also raises a variety of hypothesis. Thus, as future perspectives to help enlighten some questions that are brought up during this study, the possible beneficial impact of the conjugated therapy on migration, proliferation and angiogenic potential of EC under higher concentrations of simvastatin and under the co-treatment of rapamycin with higher doses of simvastatin, should be evaluated. The effect of these compounds, either individually or as a conjugated treatment, should also be assessed in SMC, and for that, a purer primary cell culture of SMC should be isolated. Additionally, the impact of the combined treatment in the capacity of tube formation *in vitro* could be assessed in an experimental model of co-culture with EC and SMC, in order to mimic *in vivo* environment conditions. Regarding the autophagy pathway, a proper characterisation of PAEC and SMC response to autophagy inducers and inhibitors would have to be done. To accurately characterise autophagic flux in both cell types, simvastatin incubation concomitantly with lysosome inhibition should be performed during the same period. The simvastatin effect in autophagy modulation could be more deeply analysed by taking advantage of quantitative assays to monitor autophagy in live EC and SMC. To enlighten whether simvastatin is enhancing autophagosome formation, both cell types could be transfected with a fluorescent GFP-LC3 construct to detect the presence of LC3 puncta. Moreover, cell-cell communication could be evaluated by the transfer of a fluorescent dye, for instance, giving information about Cx43 abundancy.

7. References

1. Xin, M., Olson, E. N. & Bassel-duby, R. NIH Public Access. *Nat. Rev. Mol. Cell Biol.* **14,** 529–541 (2013).

2. Martins-Marques, T. *et al.* Ischaemia-induced autophagy leads to degradation of gap junction protein connexin43 in cardiomyocytes. *Biochem. J.* **467,** 231–45 (2015).

3. Martins-Marques, T. *et al.* To beat or not to beat: degradation of Cx43 imposes the heart rhythm. *Biochem. Soc. Trans.* **43,** 476–81 (2015).

4. Waller, B. F. Anatomy, Histology, and Pathology of the Major Epicardial Coronary Arteries Relevant to Echocardiographic Imaging Techniques. *J. Am. Soc. Echocardiogr.* **2,** 232–252 (1989).

5. Bloom. in *A textbook of histology* (ed. Fawcett, D.) 394–397 (WB Saunders, 1994).

6. Virmani, R., Kolodgie, F. D., Burke, A. P., Farb, A. & Schwartz, S. M. Lessons from sudden coronary death: A comprehensive morphological classification scheme for atherosclerotic lesions. *Arterioscler. Thromb. Vasc. Biol.* **20,** 1262–1275 (2000).

7. Cahill, P. A. & Redmond, E. M. Vascular endothelium - Gatekeeper of vessel health. *Atherosclerosis* **248,** 97–109 (2016).

8. Mitchell, R. N. in *Pathologic basis of disease* (eds. Rubin, E. & Farber, J.) 483–522 (JB Lippincott, 2015). doi:10.1007/978-1-4471-6554-5_1

9. Mozaffarian, D. *et al.* Heart disease and stroke statistics-2016 update a report from the American Heart Association. *Circulation* **133,** e38–e48 (2016).

10. Sadoun, E. & Reed, M. J. Impaired Angiogenesis in Aging Is Associated with Alterations in Vessel Density , Matrix Composition , Inflammatory Response , and Growth Factor Expression. *J. Histochem. Cytochem.* **51,** 1119–1130 (2003).

11. Rocco Barazzoni, K. R. S. Effects of aging on mitochondrial. *Circ. Res.* **Biological,** 3343–3347 (2000).

12. Thijssen, D. H. J. *et al.* Haematopoietic stem cells and endothelial progenitor cells in healthy men: Effect of aging and training. *Aging Cell* **5,** 495–503 (2006).

13. Keymel, S. *et al.* Impaired endothelial progenitor cell function predicts age-dependent carotid intimal thickening. *Basic Res. Cardiol.* **103,** 582–586 (2008).

14. Ungvari, Z. *et al.* Ionizing radiation promotes the acquisition of a senescence-associated secretory phenotype and impairs angiogenic capacity in cerebromicrovascular endothelial cells: Role of increased dna damage and decreased dna repair capacity in microvascular radiosens. *Journals Gerontol. - Ser. A Biol. Sci. Med. Sci.* **68,** 1443–1457 (2013).

15. Katritsis, D. G., Mark, D. B. & Gersh, B. J. Revascularization in stable coronary disease: evidence and uncertainties. *Nat. Rev. Cardiol.* 6–9 (2018). doi:10.1038/s41569-018-0006-z

16. Arbab-Zadeh, A. & Fuster, V. The myth of the "vulnerable plaque": transitioning from a focus on individual lesions to atherosclerotic disease burden for coronary artery disease risk assessment. *J. Am. Coll. Cardiol.* **65,** 846–55 (2015).

17. Giddens, D. P., Zarins, C. K. & Glagov, S. The role of fluid mechanics in the localization and detection of atherosclerosis. *J. Biomech. Eng.* **115,** 588–94 (1993).

18. Fredrick Cornhill, J. & Roach, M. R. A quantitative study of the localization of atherosclerotic lesions in the rabbit aorta. *Atherosclerosis* **23,** 489–501 (1976).

19. Simionescu, M. Implications of early structural-functional changes in the endothelium for vascular disease. *Arteriosclerosis, Thrombosis, and Vascular Biology* **27,** 266–274 (2007).

20. Gimbrone, M. A. & García-Cardeña, G. Endothelial Cell Dysfunction and the Pathobiology of Atherosclerosis. *Circ. Res.* **118,** 620–636 (2016).

21. Libby, P., Okamoto, Y., Rocha, V. Z. & Folco, E. Inflammation in Atherosclerosis: *Circ. J.* **74,** 213–220 (2010).

22. Tabas, I., García-Cardeña, G. & Owens, G. K. Recent insights into the cellular biology of atherosclerosis. *Journal of Cell Biology* **209,** 13–22 (2015).

23. Virmani, R., Kolodgie, F. D., Burke, A. P., Farb, A. & Schwartz, S. M. Lessons From Sudden Coronary Death. *Arter. Thromb Vasc Biol.* **20,** 1262–1275 (2000).

24. Belli, A., Jackson, J. & Allison, D. in *Vascular diseases in the limbs. Mechanisms and principals of treatment* (eds. Clement, D. & Shepherd, J.) 239–58 (Mosby, 1993).

25. Iqbal, J., Gunn, J. & Serruys, P. W. Coronary stents: Historical development, current status and future directions. *British Medical Bulletin* **106,** 193–211 (2013).

26. Yahagi, K. *et al.* Pathophysiology of native coronary, vein graft, and in-stent atherosclerosis. *Nature Reviews Cardiology* **13,** 79–98 (2016).

27. Serruys, P. W. *et al.* A comparison of balloon-expandable-stent implantation with balloon angioplasty in patients with coronary artery disease. Benestent Study Group. *N.Engl.J.Med.* **331,** 489–495 (1994).

28. Costa, M. A. & Simon, D. I. Molecular basis of restenosis and drug-eluting stents. *Circulation* **111,** 2257–2273 (2005).

29. Strauss, B. H. *et al.* In vivo collagen turnover following experimental balloon angioplasty injury and the role of matrix metalloproteinases. *Circ. Res.* **79,** 541–50 (1996).

30. Tanner, F. C. *et al.* Expression of Cyclin-Dependent Kinase Inhibitors in Vascular Disease. *Circ. Res.* **82,** 396–403 (1998).

31. Pourdjabbar, A., Hibbert, B., Simard, T., Ma, X. & O'Brien, E. R. Pathogenesis of Neointima Formation Following Vascular Injury. *Cardiovasc. Hematol. Disord. Drug Targets* **11,** 30–39 (2011).

32. Fishman, J. A., Ryan, G. B. & Karnovsky, M. J. Endothelial regeneration in the rat carotid artery and the significance of endothelial denudation in the pathogenesis of myointimal thickening. *Lab Invest* **32,** 339–351 (1975).

33. Dussaillant, G. R. *et al.* Small stent size and intimal hyperplasia contribute to restenosis: A volumetric intravascular ultrasound analysis. *J. Am. Coll. Cardiol.* **26,** 720–724 (1995).

34. Otsuka, F., Nakano, M., Ladich, E., Kolodgie, F. D. & Virmani, R. Pathologic Etiologies of Late and Very Late Stent Thrombosis following First-Generation Drug-Eluting Stent Placement. *Thrombosis* **2012,** 608593 (2012).

35. Daemen, J. *et al.* Early and late coronary stent thrombosis of sirolimus-eluting and paclitaxel-eluting stents in routine clinical practice: data from a large two-institutional cohort study. *Lancet* **369,** 667–678 (2007).

36. Nebeker, J. R. *et al.* Hypersensitivity cases associated with drug-eluting coronary stents: A review of available cases from the Research on Adverse Drug Events and Reports (RADAR) project. *Journal of the American College of Cardiology* **47,** 175–181 (2006).

37. Hong, S. J. *et al.* Multiple predictors of coronary restenosis after drug-eluting stent implantation in patients with diabetes. *Heart* **92,** 1119–1124 (2006).

38. Levin, A. D., Vukmirovic, N., Hwang, C.-W. & Edelman, E. R. Specific binding to intracellular proteins determines arterial transport properties for rapamycin and paclitaxel. *Proc. Natl. Acad. Sci.* **101,** 9463–9467 (2004).

39. Endepols, H. *et al.* In vivo Molecular Imaging of Glutamate Carboxypeptidase II Expression in Re-endothelialisation after Percutaneous Balloon Denudation in a Rat Model. *Sci. Rep.* **8,** 1–7 (2018).

40. Poon, M. *et al.* Rapamycin inhibits vascular smooth muscle cell migration. *J. Clin. Invest.* **98,** 2277–2283 (1996).

41. Wiskirchen, J. *et al.* The Effects of Paclitaxel on the Three Phases of Restenosis. *Invest. Radiol.* **39,** 565–571 (2004).

42. Joner, M. *et al.* Pathology of Drug-Eluting Stents in Humans. Delayed Healing and Late Thrombotic Risk. *J. Am. Coll. Cardiol.* **48,** 193–202 (2006).

43. Marx, S. O., Jayaraman, T., Go, L. O. & Marks, A. R. Rapamycin-FKBP Inhibits Cell Cycle Regulators of Proliferation in Vascular Smooth Muscle Cells. *Circ. Res.* **76,** 412–417 (1995).

44. Dikic, I. & Elazar, Z. Mechanism and medical implications of mammalian autophagy. *Nature Reviews Molecular Cell Biology* **19,** 349–364 (2018).

45. Martinet, W. *et al.* Drug-induced macrophage autophagy in atherosclerosis: For better or worse? *Basic Research in Cardiology* **108,** 321 (2013).

46. Sadoun, E. & Reed, M. J. Impaired Angiogenesis in Aging Is Associated with

Alterations in Vessel Density, Matrix Composition, Inflammatory Response, and Growth Factor Expression. *J. Histochem. Cytochem.* **51,** 1119–1130 (2003).

47. Ungvari, Z. *et al.* Endothelial dysfunction and angiogenesis impairment in the ageing vasculature. *Nature Reviews Cardiology* 1–11 (2018). doi:10.1038/s41569-018-0030-z

48. Bar-Peled, L. & Sabatini, D. M. Regulation of mTORC1 by amino acids. *Trends in Cell Biology* **24,** 400–406 (2014).

49. Kim J, Kundu M, Viollet B, G. K. MPK and mTOR regulate autophagy through direct phosphorylation of Ulk1. *Nat Cell Biol.* **13,** 132–141 (2011).

50. Manuscript, A., Receptors, U. & Control, P. Q. NIH Public Access. *J Mol Cell Cardiol* 73–84 (2014). doi:10.1016/j.yjmcc.2012.09.012.Ubiquitin

51. Herzig, S. & Shaw, R. J. AMPK: Guardian of metabolism and mitochondrial homeostasis. *Nature Reviews Molecular Cell Biology* **19,** 121–135 (2018).

52. Severs, N. J. *et al.* Immunocytochemical analysis of connexin expression in the healthy and diseased cardiovascular system. *Microsc. Res. Tech.* **52,** 301–322 (2001).

53. González, A. & Hall, M. N. Nutrient sensing and TOR signaling in yeast and mammals. *EMBO J.* **36,** 397–408 (2017).

54. Meley, D. *et al.* AMP-activated protein kinase and the regulation of autophagic proteolysis. *J. Biol. Chem.* **281,** 34870–34879 (2006).

55. Inoki, K., Zhu, T. Q. & Guan, K. L. TSC2 mediates cellular energy response to control cell growth and survival. *Cell* **115,** 577–590 (2003).

56. Lesniewski, L. A., Zigler, M. C., Durrant, J. R. & Donato, A. J. Sustained Activation of AMPK Ameliorates Age-Associated Vascular Endothelial Dysfunction via a Nitric Oxide-Independent Mechanism. *Mech Ageing Dev.* **133,** 368–371 (2013).

57. Birgisdottir, B., Lamark, T. & Johansen, T. The LIR motif – crucial for selective autophagy. *J. Cell Sci.* **126,** 3237–3247 (2013).

58. Mauvezin, C. & Neufeld, T. P. Bafilomycin A1 disrupts autophagic flux by inhibiting both V-ATPase-dependent acidification and Ca-P60A/SERCA-dependent autophagosome-lysosome fusion. *Autophagy* **11,** 1437–1438 (2015).

59. De Meyer, G. R. Y. *et al.* Autophagy in vascular disease. *Circulation Research* **116,** 468–479 (2015).

60. Schrijvers, D. M., De Meyer, G. R. Y. & Martinet, W. Autophagy in atherosclerosis: A potential drug target for plaque stabilization. *Arterioscler. Thromb. Vasc. Biol.* **31,** 2787–2791 (2011).

61. Grootaert, M. O. J. *et al.* Defective autophagy in vascular smooth muscle cells accelerates senescence and promotes neointima formation and atherogenesis. *Autophagy* **11,** 2014–2032 (2015).

62. Martinet, W. & De Meyer, G. R. Y. Autophagy in atherosclerosis: A cell survival and death phenomenon with therapeutic potential. *Circulation Research* **104,** 304–317 (2009).

63. Jia, G., Cheng, G. & Agrawal, D. K. Autophagy of vascular smooth muscle cells in atherosclerotic lesions. *Autophagy* **3,** 63–64 (2007).

64. He, C. *et al.* 7-ketocholesterol induces autophagy in vascular smooth muscle cells through Nox4 and Atg4B. *Am. J. Pathol.* **183,** 626–637 (2013).

65. Zhao, H. Q., Nikanorov, A., Virmani, R. & Schwartz, L. B. Inhibition of experimental neointimal hyperplasia and neoatherosclerosis by local, stent-mediated delivery of everolimus. *J. Vasc. Surg.* **56,** 1680–1688 (2012).

66. Hayashi, S. I. *et al.* The stent-eluting drugs sirolimus and paclitaxel suppress healing of the endothelium by induction of autophagy. *Am. J. Pathol.* **175,** 2226–2234 (2009).

67. Mihos, C. G., Salas, M. J. & Santana, O. The pleiotropic effects of the hydroxy-methyl-glutaryl-CoA reductase inhibitors in cardiovascular disease: A comprehensive review. *Cardiology in Review* **18,** 298–304 (2010).

68. Vaughan, C. J., Gotto, A. M. & Basson, C. T. The evolving role of statins in the management of atherosclerosis. *Journal of the American College of Cardiology* **35,** 1–10 (2000).

69. Kreisberg, R. A. Reductase inhibitor therapy of hypercholesterolemia. *Trans. Am. Clin. Climatol. Assoc.* **102,** 153-63–5 (1991).

70. Fears, R., Richards, D. H. & Ferres, H. The effect of compactin, a potent inhibitor of 3-hydroxy-3-methylglutaryl coenzyme-A reductase activity, on cholesterogenesis and serum cholesterol levels in rats and chicks. *Atherosclerosis* **35,** 439–449 (1980).

71. Fukuda, D., Enomoto, S., Shirakawa, I., Nagai, R. & Sata, M. Fluvastatin accelerates re-endothelialization impaired by local sirolimus treatment. *Eur. J. Pharmacol.* **612,** 87–92 (2009).

72. Echeverri, D. & Cabrales, J. Statins and percutaneous coronary intervention: A complementary synergy. *Clinica e Investigacion en Arteriosclerosis* **25,** 112–122 (2013).

73. Lidington, E. A. *et al.* Conditional immortalization of growth factor-responsive cardiac endothelial cells from H-2K(b)-tsA58 mice. *Am. J. Physiol. Cell Physiol.* **282,** C67–C74 (2002).

74. Brisset, A. C., Isakson, B. E. & Kwak, B. R. Connexins in Vascular Physiology and Pathology. *Antioxid. Redox Signal.* **11,** 267–282 (2009).

75. Severs, N. J. *et al.* Immunocytochemical Analysis of Connexin Expression in the Healthy and Diseased Cardiovascular System. *Microsc. Res. Tech.* **322,** 301–322 (2001).

76. Han, X. J. *et al.* Lentivirus-mediated RNAi knockdown of the gap junction protein, Cx43, attenuates the development of vascular restenosis following balloon injury. *Int. J. Mol. Med.* **35,** 885–892 (2015).

77. Déglise, S. *et al.* Increased connexin43 expression in human saphenous veins in culture is associated with intimal hyperplasia. *J. Vasc. Surg.* **41,** 1043–1052 (2005).

78. Liu, H. *et al.* Rapamycin Inhibits Re-Endothelialization after Percutaneous Coronary Intervention. *Tex Hear. Inst J* **37,** 194–201 (2010).

79. Matter, C. M. *et al.* Effects of tacrolimus or sirolimus on proliferation of vascular smooth muscle and endothelial cells. *J. Cardiovasc. Pharmacol.* **48,** 286–292 (2006).

80. Parry, T. J. *et al.* Drug-eluting stents: Sirolimus and paclitaxel differentially affect cultured cells and injured arteries. *Eur. J. Pharmacol.* **524,** 19–29 (2005).

81. Jaschke, B. *et al.* Local statin therapy differentially interferes with smooth muscle and endothelial cell proliferation and reduces neointima on a drug-eluting stent platform. *Cardiovasc. Res.* **68,** 483–492 (2005).

82. Pan, Q., Xie, X., Guo, Y. & Wang, H. Simvastatin promotes cardiac microvascular endothelial cells proliferation, migration and survival by phosphorylation of p70 S6K and FoxO3a. *Cell Biol. Int.* **38,** 599–609 (2014).

83. Urbich, C., Dernbach, E., Zeiher, A. M. & Dimmeler, S. Double-edged role of statins in angiogenesis signaling. *Circ. Res.* **90,** 737–744 (2002).

84. Weis, M., Heeschen, C., Glassford, A. J. & Cooke, J. P. Statins have biphasic effects on angiogenesis. *Circulation* **105,** 739–745 (2002).

85. Kureishi, Y. *et al.* NIH Public Access. *Nat Med* **6,** 1004–1010 (2010).

86. Ii, M. & Losordo, D. W. Statins and the endothelium. *Vascular Pharmacology* **46,** 1–9 (2007).

87. Ravikumar, B. *et al.* Inhibition of mTOR induces autophagy and reduces toxicity of polyglutamine expansions in fly and mouse models of Huntington disease. *Nat. Genet.* **36,** 585–595 (2004).

88. Tanida, I., Ueno, T. & Kominami, E. LC3 and autophagy. *Methods Mol. Biol.* **445,** 77–88 (2008).

89. Huang, R. & Liu, W. Identifying an essential role of nuclear LC3 for autophagy. *Autophagy* **11,** 852–853 (2015).

90. Bejarano, E. *et al.* Autophagy modulates dynamics of connexins at the plasma membrane in a ubiquitin-dependent manner. *Mol. Biol. Cell* **23,** 2156–2169 (2012).

91. Lichtenstein, A., Minogue, P. J., Beyer, E. C. & Berthoud, V. M. Autophagy: a pathway that contributes to connexin degradation. *J. Cell Sci.* **124,** 910–920 (2011).

92. Andres, A. M. *et al.* Mitophagy Is Required for Acute Cardioprotection by

Simvastatin. *Antioxid. Redox Signal.* **21,** 1960–1973 (2014).

93. Parikh, A. *et al.* Statin-induced autophagy by inhibition of geranylgeranyl biosynthesis in prostate cancer PC3 cells. *Prostate* **70,** 971–981 (2010).

94. Araki, M., Maeda, M. & Motojima, K. Hydrophobic statins induce autophagy and cell death in human rhabdomyosarcoma cells by depleting geranylgeranyl diphosphate. *Eur. J. Pharmacol.* **674,** 95–103 (2012).

95. Huang, B. *et al.* Simvastatin enhances oxidized-low density lipoprotein-induced macrophage autophagy and attenuates lipid aggregation. *Mol. Med. Rep.* **11,** 1093–1098 (2015).

96. Zhang, Q. *et al.* Autophagy Activation: A Novel Mechanism of Atorvastatin to Protect Mesenchymal Stem Cells from Hypoxia and Serum Deprivation via AMP-Activated Protein Kinase/Mammalian Target of Rapamycin Pathway. *Stem Cells Dev.* **21,** 1321–1332 (2012).

97. Tziakas, D. N. *et al.* Statin use is associated with a significant reduction in cholesterol content of erythrocyte membranes. A novel pleiotropic effect? *Cardiovasc. Drugs Ther.* **23,** 471–480 (2009).

98. Xu, J., Dang, Y., Ren, Y. R. & Liu, J. O. Cholesterol trafficking is required for mTOR activation in endothelial cells. *Proc. Natl. Acad. Sci.* **107,** 4764–4769 (2010).

99. Simons, K. & Ikonen, E. Functional Rafts in Cell-Membranes. *Nature* **387,** 569–572 (1997).

100. Brown, M. S. & Goldstein, J. L. M58 A receptor-mediated pathway for cholesterol homeostasis. *Science* **232,** 34–47 (1986).

101. Bloch, K. The Biological Synthesis of Cholesterol. *Science (80-.).* **150,** 19–28 (1965).

102. Ranieri, R. *et al.* N6-isopentenyladenosine dual targeting of AMPK and Rab7 prenylation inhibits melanoma growth through the impairment of autophagic flux. *Cell Death Differ.* **25,** 353–367 (2018).